



## Cronfa - Swansea University Open Access Repository

---

This is an author produced version of a paper published in:  
*Biochimica et Biophysica Acta (BBA) - Molecular and Cell Biology of Lipids*

Cronfa URL for this paper:  
<http://cronfa.swan.ac.uk/Record/cronfa41148>

---

### Paper:

Zhou, W., Warrilow, A., Thomas, C., Ramos, E., Parker, J., Price, C., Vanderloop, B., Fisher, P., Loftis, M., et. al. (2018). Functional importance for developmental regulation of sterol biosynthesis in *Acanthamoeba castellanii*. *Biochimica et Biophysica Acta (BBA) - Molecular and Cell Biology of Lipids*, 1863(10), 1164-1178.  
<http://dx.doi.org/10.1016/j.bbalip.2018.07.004>

Released under the terms of a Creative Commons Attribution Non-Commercial No Derivatives License (CC-BY-NC-ND).

---

This item is brought to you by Swansea University. Any person downloading material is agreeing to abide by the terms of the repository licence. Copies of full text items may be used or reproduced in any format or medium, without prior permission for personal research or study, educational or non-commercial purposes only. The copyright for any work remains with the original author unless otherwise specified. The full-text must not be sold in any format or medium without the formal permission of the copyright holder.

Permission for multiple reproductions should be obtained from the original author.

Authors are personally responsible for adhering to copyright and publisher restrictions when uploading content to the repository.

<http://www.swansea.ac.uk/library/researchsupport/ris-support/>

1  
2  
3  
4  
5  
6  
7  
8  
9  
10  
11  
12  
13  
14  
15  
16  
17  
18  
19  
20  
21  
22  
23  
24  
25  
26  
27  
28

Classification: Biological Sciences, Biochemistry

**Functional Importance for Developmental Regulation of Sterol Biosynthesis in  
*Acanthamoeba castellanii***

Wenxu Zhou<sup>1±</sup>, Andrew G.S. Warrilow,<sup>2±</sup> Crista D. Thomas<sup>1±</sup>, Emilio Ramos,<sup>1</sup> Josie E. Parker,<sup>2</sup>  
Claire L. Price,<sup>2</sup> Boden H. Vanderloop,<sup>1</sup> Paxtyn M. Fisher,<sup>1</sup> Michael D. Loftis,<sup>1</sup> Diane E. Kelly,<sup>2</sup>  
Steven L. Kelly<sup>2</sup>, and W. David Nes<sup>1\*</sup>

<sup>1</sup>Department of Chemistry and Biochemistry, Texas Tech University, Lubbock, Texas, United States of America

<sup>2</sup>Center for Cytochrome P450 Biodiversity, Institute of Life Science, College of Medicine, Swansea University, Swansea, Wales, United Kingdom

\*Corresponding author: W. David Nes, Department of Chemistry & Biochemistry, Texas Tech University, Lubbock, Texas, USA 79424, E-mail: wdavid.nes@ttu.edu (WDN)

<sup>±</sup>These authors contributed equally to this work.

## 29 Abstract

30 The sterol metabolome of *Acanthamoeba castellanii* (Ac) yielded 25 sterols. Substrate screening  
31 of cloned AcCYP51 revealed obtusifoliol as the natural substrate which converts to  $\Delta^{8,14}$ -sterol  
32 (<95%). The combination of [ $^2\text{H}_3$ -methyl]methionine incubation to intact cultures showing C<sub>28</sub>-  
33 ergosterol incorporates 2- $^2\text{H}$  atoms and C<sub>29</sub>-7-dehydroporiferasterol incorporates 5  $^2\text{H}$ -atoms, the  
34 natural distribution of sterols, CYP51 and previously published sterol methyltransferase (SMT)  
35 data indicate separate  $\Delta^{24(28)}$  - and  $\Delta^{25(27)}$  -olefin pathways to C<sub>28</sub>- and C<sub>29</sub>- sterol products from  
36 the protosterol cycloartenol. In cell-based culture, we observed a marked change in sterol  
37 compositions during the growth and encystment phases monitored microscopically and by trypan  
38 blue staining; trophozoites possess C<sub>28</sub>/C<sub>29</sub>- $\Delta^{5,7}$ -sterols, viable encysted cells (mature cyst)  
39 possess mostly C<sub>29</sub>- $\Delta^5$ -sterol and non-viable encysted cells possess C<sub>28</sub>/C<sub>29</sub>- $\Delta^{5,7}$ -sterols that  
40 turnover variably from stress to 6-methyl aromatic sterols associated with changed membrane  
41 fluidity affording lysis. An incompatible fit of steroidal aromatics in membranes was confirmed  
42 using the yeast sterol auxotroph GL7. Only viable cysts, including those treated with inhibitor,  
43 can excyst into trophozoites. 25-Azacycloartanol or voriconazole that target SMT and CYP51,  
44 respectively, are potent enzyme inhibitors in the nanomolar range against the cloned enzymes  
45 and amoeba cells. At minimum amoebicidal concentration of inhibitor amoeboid cells rapidly  
46 convert to encysted cells unable to excyst. The correlation between stage-specific sterol  
47 compositions and the physiological effects of ergosterol biosynthesis inhibitors suggests that  
48 amoeba fitness is controlled mainly by developmentally-regulated changes in the phytosterol B-  
49 ring; paired interference in the  $\Delta^{5,7}$ -sterol biosynthesis (to  $\Delta^{5,7}$ ) - metabolism (to  $\Delta^5$  or 6-methyl  
50 aromatic) congruence during cell proliferation and encystment could be a source of therapeutic  
51 intervention for *Acanthamoeba* infections

52 Key words: *Acanthamoeba castellanii*, sterol methyltransferase, sterol evolution, aromatic  
53 sterols, trophozoite, encystment, ergosterol biosynthesis inhibitor

54

55 Abbreviations: Ac, *Acanthamoeba castellanii*, SMT, sterol methyl transferase, GC-MS, gas-  
56 chromatography-mass spectroscopy, VOR, voriconazole, AZC, 25-azacycloartanol, RRTc,  
57 retention time of unknown to retention time of cholesterol in GC. Mya, million years ago.

58 Highlights:

- 59 1. *Acanthamoeba castellanii* cells generate 25 sterols, a mixture of 4-methyl intermediates  
60 and  $\Delta^5$ -final products, affording a biosynthetic pathway recurrent from an ancient algal  
61 predecessor; separate intermediates via the  $\Delta^{24(28)}$  -methyl olefin route and  $\Delta^{25(27)}$  - ethyl  
62 olefin route determine the C<sub>28</sub>- and C<sub>29</sub>-sterol balance in the amoeba.
- 63 2. Cloned AcCYP51 favors obtusifoliol as substrate, but can convert cycloeucaenol weakly  
64 to  $\Delta^{14}$ -product.
- 65 3.  $\Delta^{5,7}$  - and  $\Delta^5$ -sterols are differentially correlated to trophozoite growth and mature cyst  
66 viability and excystment, respectively, while 6-methyl aromatic sterols are a chemical  
67 signature indicative of encysted cells on the path to death.
- 68 4. Voriconazole inhibits AcCYP51 as other azoles and 25-azacycloartanol inhibits AcSMT  
69 in the low nanmolar range; these drugs are potent inhibitors of trophozoite growth and  
70 impair encystment toward viable cyst production in the range of 500 nM to 3  $\mu\text{M}$ .

## 71 1. Introduction

72 Sterol synthesis is a basic metabolic pathway of eukaryotes giving rise to essential membrane  
73 components. The biosynthesis pathway is typically divided into three routes, two of which  
74 characterize the phytosterol biosynthesis pathways in land plants and fungi yielding C<sub>29</sub>-  
75 sitosterol (24 $\alpha$ -ethyl group) and C<sub>28</sub>-ergosterol (24 $\beta$ -methyl group), respectively, and in animals  
76 yielding C<sub>27</sub>-cholesterol (Fig. 1) [1-4]. These contemporary biosynthetic pathways retain  
77 ancestral features along with novelties specific to their particular lineages. Notably, the  
78 protosterol product of the 2,3-oxidosqualene synthase yielding cycloartenol or lanosterol  
79 associates phylogenetically to plant-animal divisions while the substrate acceptability and  
80 mechanisms of individual enzymes catalyzing completion of the pathway to  $\Delta^5$ -sterols reveal  
81 relatedness or divergence in catalytic competence across kingdoms [5, 6]. For phytosterols  
82 generating diversity, the size, location and direction ( $\alpha$ - or  $\beta$ -orientation) of the side chain C<sub>24</sub>-  
83 alkyl group correlate to plant-fungal divisions or to more- or less-advanced in descent. Structural  
84 features common to sterols are a cyclopentanoperhydrophenanthrene ring system, polar C<sub>3</sub>-OH  
85 group and intact side chain of 8 to 10-carbon atoms. These characteristics contribute positively to  
86 the molecule's overall flat shape, length and amphipathic character relevant to the architectural  
87 suitability of sterols in membranes [7]. Alternatively, there can be harmful features in  
88 intermediates that are removed during the normal course of metabolism. For example, the C<sub>4</sub>-  
89 geminal methyl groups and C<sub>14</sub>-methyl group on the protosterol, eliminated to yield  $\Delta^5$ -sterols,  
90 are known to affect the hydrogen bonding strength of the C<sub>3</sub>-OH group and planarity of the  $\alpha$ -  
91 (back) face of the sterol nucleus, respectively; when intermediates that possess these features  
92 accumulate in the cell the result can be detrimental to sterol homeostasis that thereby, interferes  
93 with growth and maturation [8-10].

94 Despite the prevailing hypothesis suggesting progressive structural modifications in the  
95 protosterol formed by prokaryotes parallels a gradual cholesterol evolution in response to  
96 increases in the atmospheric concentration of oxygen [11-13] recent chemical analysis on the  
97 origin of these compounds indicate a complete sterol biosynthesis to  $\Delta^5$ -products may have  
98 existed in the most primitive eukaryotes, evidenced in the presence of cholestane and its C<sub>28</sub>- to  
99 C<sub>30</sub>-carbon homologs in molecular fossils found in rocks and formations between 750 Mya to  
100 1,000 Mya [14]. Additionally, phylogenomic analysis shows the genes of 13 sterolic enzymes

101 yielding these steranes could be codified in the genomic organization of the last eukaryotic  
102 common ancestor (LECA) approximately 2.45-2.32 Mya [15, 16] with orthologous prokaryotic  
103 enzymes likely formed during the Great Oxidation Event by horizontal gene transfers [17, 18].  
104 Based on this new information, we surmise competing phylogenies constructed from these  
105 characters could reasonably describe the punctuated and recurrent evolution of sterol  
106 biosynthesis to amoeba ergosterol deeply rooted in primary metabolism of the LECA [19, 20].  
107 However, relevant to the understanding of sterol biosynthesis in *Acanthamoeba* for the purpose  
108 of inhibition, the phyla-specific canonical routes to alternate sterol products must also be  
109 considered, because different steps in sterol metabolism – sterol side chain or nucleus revisions-  
110 could interface uniquely through stage-specific structural adjustment during the amoeba life  
111 history, as reported can occur in land plants [21, 22] to yield ergosterol convergence (Fig. 1).

112 *Acanthamoeba* spp. has a number of particularly advantageous characteristics for research on  
113 sterol function and evolution. In the first place, the differentiation process originating in the  
114 trophozoite and passing through a pseudocyst, i.e., an intermediate structure composed of a wall  
115 that may not protect against adverse conditions [23, 24], can yield multiple cyst types, including  
116 1) *viable* cysts with a resistant double-layered outer wrinkled ectocyst and inner endocyst and 2)  
117 a mixture of *non-viable* cysts of apoptotic cells that possess a fragile cell wall and dead cells  
118 generated from autophagocytosis [25]. These studies further show azolic inhibitors-voriconazole  
119 can prevent trophozoite growth as well as activate an encystment pathway with a final trajectory  
120 ending in programmed cell death [26]. Ergosterol biosynthesis inhibitors with various structures  
121 can therefore be administered and the effects on growth and differentiation measured in  
122 correlation to changes in sterol biosynthesis. Intriguingly, the unikont *Acanthamoeba* is distinctly  
123 different from fungi and bikont protozoa (kinetoplastids) in their sterol biosynthesis capabilities.  
124 The variant pathways for C<sub>28</sub>-ergosterol biosynthesis in parasitic protozoa also differ from the  
125 C<sub>27</sub>-cholesterol biosynthesis in the human host where sterol C<sub>24</sub>-methylation is lost [27].

126 The ability of *Acanthamoeba* spp to synthesize a plant-based pathway of cycloartenol to  $\Delta^5$ - and  
127  $\Delta^{5,7}$ -24 $\beta$ -C<sub>28</sub>- and C<sub>29</sub>-alkyl sterols was discovered in the early 1980's by Raedorstorff and  
128 Rohmer [28, 29]. These researchers together with the Korn group demonstrated the amoeba  
129 ergosterol and 7-dehydroporiferasterol can convert to uncommon C<sub>28</sub> - and C<sub>29</sub>-phenanthrene 6-  
130 methyl aromatic sterols [30, 31]. The *Acanthamoeba* system has been exploited in the

131 collaborative laboratories of Kelly and Nes [32, 33] and more recently by Roberts and coworkers  
132 [34]. However, unlike the Rohmer and Korn groups, the more recent authors [34] have  
133 concluded that *Acanthamoeba* operates a fungal-based pathway of lanosterol to ergosterol and  
134 the protozoan is unable to synthesize C<sub>29</sub>-sterols. Our own preliminary work corroborated the  
135 original findings, and the purpose of the present paper is to document this in detail and to expand  
136 the study to encompass a more comprehensive evaluation of the biosynthetic enzymes and  
137 steroidal nuggets expressed variably at stage-specific times in *Acanthamoeba*. The approach used  
138 in our investigation has been chosen to validate the ergosterol biosynthesis pathway from  
139 cycloartenol and the existence of a new  $\Delta^{25(27)}$ -C<sub>29</sub>-sterol biosynthesis pathway in amoeba that  
140 recapitulates the green algal sterol biosynthesis pathway to C<sub>29</sub>-sterols.

141 Another reason for choosing *Acanthamoeba* was the critical factors in target deconvolution using  
142 sterolomics, bioinformatics and genetic technologies that led to enzyme-based strategies for  
143 manipulating the ergosterol biosynthesis pathway in this and related parasitic protozoa. These  
144 various investigations provide new chemical starting points against our target enzymes- the  
145 *Acanthamoeba castellanii* (Ac) sterol C14-demethylase (CYP51) and sterol C24/C28-  
146 methyltransferases (SMT). Inhibition of either enzyme by a rationally designed tight binding  
147 inhibitor rapidly yields trophozoite death [33]. The only real uncertainties left about the  
148 importance of phytosterol biosynthesis/metabolism in *Acanthamoeba* are: (i) can the sterol  
149 composition change during the amoeba life cycle, (ii) has phylogenetics influenced formation of  
150 separate routes to C<sub>28</sub>- and C<sub>29</sub>-sterols, (iii) to what extent is ergosterol biosynthesis during the  
151 *Acanthamoeba* encystment-excystment cycle vulnerable to inhibitors and (iv) what role is played  
152 in *Acanthamoeba* physiology by changing the sterol B-ring structure from  $\Delta^{5,7}$  - to  $\Delta^5$  - or 6-  
153 methyl aromatic group?

154 In this study, the pattern of sterol biosynthesis and accumulation in *Acanthamoeba* against  
155 ultrastructure and viability of the cells was determined at various stages of amoeba proliferation  
156 and encystment. In addition, we examined the physiological role of the uncommon 6-methyl  
157 aromatic sterol structures generated by the amoeba through use of enzyme inhibitors and the  
158 yeast sterol auxotroph GL7. The results define the biosynthetic factors that control the changes in  
159 sterol compositions associated with amoeba differentiation, and provide the necessary foundation  
160 for further regulatory studies at the biochemical and molecular levels. Given the therapeutic

161 importance for CYP51 and SMT as chokepoint enzymes in Acanthamoeba and other parasitic  
162 protozoa, knowledge of the diversity and function of terminal C<sub>28</sub>- and C<sub>29</sub>-sterols in the  
163 trophozoite and encysted cell can be of value in developing new inhibitor chemotypes to treat  
164 amoeba diseases.

165

166

167

168

169

170

171

172

173

174

175

176

177

178

179

180

181

182

183

184

185

186

187

188

189

190        **2. Materials and methods**

191    *2.1. Strain and culture conditions.* *Acanthamoeba castellanii* strain ATCC 30010 was inoculated  
192 into tissue culture 25 ml T-flasks prepared with ATTC media 712. Cells were cultured axenically  
193 in 5 ml static culture at 25 °C with occasional hand shaking to keep cells in suspension.  
194 Continuous cultures were maintained by subculture of 4-5 day growth arrested cells into fresh  
195 medium. Growth experiments to establish the growth curve and for sterol analyses were typically  
196 carried out using  $1 \times 10^4$  trophozoites (< 90%) or cysts derived by the methods below. The  
197 number of individual amoeba distinct from encysted cells that possess a double wall per ml was  
198 determined microscopically. For cell aggregates a best effort was made to count the number of  
199 individual encysted cells in the clump. Morphological changes and encystation ratios were  
200 calculated by counting trophozoite to cysts using a Neubauer hemocytometer under an Olympus  
201 CH-2 compound light microscope and in separate observations cell differentiation was detected  
202 with an inverted microscope monitored daily for 2 weeks. Cells were pelleted by centrifugation  
203 for 5 min at 5,000 g. Cell viability was checked by trypan blue exclusion method.

204    *2.2. Induction of encystment.* To generate viable cysts capable of excystment, equivalent to  
205 resting or dormant cysts, three different approaches were employed. Method-1, using wild-type  
206 trophozoites, encystment was induced naturally by allowing the early growth arrested cultures  
207 (ca. 4-5 day synchronous cultures) to deplete essential growth nutrients required in metabolite  
208 biosynthesis. In a second approach encystment was forced by two replacement methods.  
209 Method-2 is salt- induced encystment and was used by Korn et al. and Mehdi and Garg [24, 30,  
210 35]. Briefly, trophozoites were resuspended in medium containing 1 mM MgCl<sub>2</sub> to a cell  
211 concentration of approximately  $6.5 \times 10^6$  cells/ml. The culture was incubated in a 30 °C shaker at  
212 150 rpm for 2 days. The cells were collected and treated with 1% sodium dodecyl sulfate (SDS)  
213 solution for 30 min at room temperature to remove trophozoites, fragile encysted cells and cell  
214 debris. The resulting SDS-resistant cysts were washed with PAGE's saline solution 5 times and  
215 analyzed for sterols. Method 3 is starvation-induced encystment where the amoebae are  
216 maintained on an agar-embedment system for 2-4 weeks [23]. Encystment synchrony was  
217 evaluated morphologically using a combination of inverted microscopy, light microscopy and  
218 electron microscopy. More than 90-95% of the cells formed from these conditions yielded  
219 encysted cells with features representative of resting or dormant cysts. Resting cysts generated



220 by the natural and replacement methods were determined viable by their  $\Delta^5$ -sterol profile, and in  
221 each case yielded similar excystment activities of about 100%. Typically, the viable cysts at the  
222 end of these experiments appeared as single cells in light microscopy either on the solid or in  
223 liquid medium. A third approach was used to promote encystment by administering drugs to the  
224 medium.

225 *2.3. Trophozoite toxicity assay.* To determine the effect of the test compounds on the growth of  
226 *Acanthamoeba*, trophozoites, approximately  $1 \times 10^5$  cells, were inoculated into 24 well (4 x 6)  
227 microtiter plates of 3 ml final volume taking the inoculum from cells grown in the T-flask  
228 continuous culture system. Stock inhibitor concentrations were prepared in dimethylsulfoxide  
229 (not to exceed 1% solvent) and as relevant serially diluted to final concentrations in wells that  
230 ranged from 16 nM to 30  $\mu$ M (approximate to the end point for inhibitor studies administered to  
231 human epithelial kidney cells [32, 33]. Control wells containing medium and 1% DMSO solvent  
232 had no effect on the cell growth. The microliter plates were incubated at 25-<sup>0</sup>C for 48 hr and the  
233 resulting number of trophozoites to cysts counted at the end of the incubation using the  
234 hemocytometer. The percentage of viable tophozoites following to different concentrations of  
235 inhibitors was determined by the trypan blue exclusion method. The 50% effective does (IC<sub>50</sub>)  
236 value of inhibitors against tophozoite growth under the stated assay conditions was determined  
237 by linear extrapolation using GraphPad Prism (GraphPad Software Inc., CA). Cells stained blue  
238 were considered non-viable while live cells were unstained. These experiments were carried out  
239 in triplicate and at different time points. The drug concentration responsible for the minimum  
240 ameobacidal activity (MAC) was defined as the lowest concentration of the inhibitor with no  
241 visible live trophozoites, as determined by visual inspection of the treated cultures using the light  
242 microscope following trypan blue staining and inverted microscope which confirmed cell death  
243 by the absence of trophozoite cells and notable accumulation of cell debris. Observations were  
244 performed in triplicate x 2 using light microscope for counting cells. There was excellent  
245 agreement ( $\leq 10\%$  variation for any data point) in the growth response to inhibitors in the two  
246 independent trials.

247 *2.4. Time-dependent killing.* A log-phase culture of Trophozoites was seeded into 24-well plates  
248 as described above. Cells were then challenged with inhibitors at previously determined MAC  
249 concentrations. At 12 hr intervals, aliquots were removed and counted and cell viability

250 determined; at 48 hr remaining cells were pelleted and resuspended into fresh medium and  
251 allowed to incubate for another 5 days and the cells counted to determine trophozoite  
252 proliferation and analyzed for sterol content. Experiments were performed with biological  
253 replicates. A metabolic marker was used to assess viable cells by means of GC-MS analysis.  
254 Viable trophozoites were associated with the production of ergosterol/7-dehydroporiferaterol  
255 and viable cysts were associated with poriferasterol production and cells in the death mode were  
256 associated with steroidal aromatics as discussed in the text.

257 *2.5. Cysticidal assay.* Cysts, generated by the methods above, or derived from inhibitor  
258 treatment, were incubated with the anti-amoeba drug under the same assay conditions described  
259 for ameobacidal assay. Growth was defined as the presence of excysted trophozoites found  
260 growing in 24 well plates or 5 ml T-flasks after 5 days of growth.

261 *2.6. Chemical and instrumental analysis.* The source of sterol substrates and steroidal inhibitors  
262 evaluated in this study is described in earlier papers [8, 20, 36]. Voriconazole was purchased  
263 from Sigma. All sterols were purified by HPLC to < 95% by GC analysis. S-adenosyl-L-  
264 methionine (SAM) chloride salt was purchased from Sigma, [*methyl*-<sup>3</sup>H<sub>3</sub>]SAM (specific activity  
265 10-15 Ci/mMol, and diluted to 10 μCi/μMol, tetraosylate (*methyl*-<sup>2</sup>H<sub>3</sub>]SAM (99% atom  
266 enrichment) purchased from S/D/N isotopes (Pointe-Claire, QC), L-[*methyl*-<sup>2</sup>H<sub>3</sub>]methionine  
267 (Sigma). The Bradford protein assay kit was purchased from Bio-Rad and isopropyl-1-thio-β-D-  
268 galactoside (IPTG) purchased from Research Products International Corp. DNA synthesis  
269 inhibitor 5-fluor-2-deoxyuridine (FUdR) was purchased from MP Biomedicals LLC. All other  
270 reagents and chemical were from Sigma or Fisher unless otherwise noted.

271 Instrumental methods have been reported previously [19, 20]. Briefly, <sup>1</sup>H-NMR spectra were  
272 recorded in CDL<sub>3</sub> at ambient temperature using a Varian Unity Inova 500 MHz spectrometer;  
273 chemical shifts (δ, ppm) are referenced to chloroform, (δ, 7.26 ppm). Mass spectra were obtained  
274 on a Hewlett-Packard 6890 GC-HP 5973 MSD instrument (electron impact, 70eV, scan range  
275 50-550 amu). HPLC was carried out at room temperature using a Phenomenex Luna C18-column  
276 (250 mm x 4.6. mm x 5 μM) connected to a diode array multiple wavelength diode array detector  
277 with methanol as eluent. Capillary GC (0.25 mm i.d, by 30 m fused silica column coated with  
278 Zebron ZB-5 from Phenomenex) was operated at a flow rate of He set at 1.2 ml/min, injector  
279 port at 250 0C, and temperature program of initial 170 0C, held for 1 min, and increased at 20

280  $^{\circ}\text{C}/\text{min}$  to  $280^{\circ}\text{C}$ . GC analysis of sterols is reported as RRTc values referring to the retention  
281 time of sample GC peak to retention time of cholesterol peak which moved typically in the  
282 chromatogram at 13.8 min or slightly different to 14.5 min depending on whether the column tip  
283 was clipped due to age issues. In HPLC samples were separated on a Phenomenex Luna C<sub>18</sub>-  
284 column (250 mm x 4.6 mm x 5 cm) connected to a diode array multiple detector with samples  
285 eluted with methanol; the  $\alpha\text{c}$  of the sterol is the elution time of compound relative to the elution  
286 time of cholesterol, which is 20.6 min. In sterol analysis, product distributions were determined  
287 by approximate integration of chromatographic peaks, experiments were performed in biological  
288 replicates with excellent agreement between trials (>95%). Thin layer chromatography was  
289 performed on 10 x 20 cm, 250  $\mu\text{M}$  silica plates (Baker) developed twice in benzene-ether (85/15,  
290 v/v).

291 *2.7. Cell metabolite identification.* Typically, small-scale amoeba cultures were harvested  
292 different points along the growth curve in the presence and absence of steroidal inhibitor and  
293 azole at MAC concentrations of the compound. Control or treated cultures in 5 ml or 10 ml  
294 medium dispersed in 25 ml T-flasks were inoculated with trophozoites (90%) or resting cysts  
295 (100%) and cultured for the desired time without shaking and sterol analyzed at the end of the  
296 incubation period. Independently, trophozoites were incubated in the 24-well plate system  
297 containing 1 ml total medium and after 48 h treatment the sterol composition determined by GC-  
298 MS analysis. Cell pellets were split with an internal standard of  $5\alpha$ -cholestane added to one of  
299 the cell pellets for determination of sterol amounts in cells. Cells were saponified with 10%  
300 methanolic KOH extracted with hexanes and the neutral lipids routinely analyzed by GC-MS for  
301 structure determination and quantification. Components were identified by comparison of  
302 retention times in GC and HPLC and mass spectra with authentic standards in our own collection  
303 [19, 20, 22, 37] and were quantified by comparison of detector response with that of the internal  
304 standard. As relevant preparative scale incubation were carried to obtain a subset of amoeba  
305 sterols for  $^1\text{H}$ NMR analysis.

306 *2.8. Scanning (SEM) and transmission (TEM) electron microscopy.* SEM: Prior to fixation,  
307 control and treated cell pellets were rinsed in 10% phosphate buffer solution, and centrifuged  
308 again to remove any salts that would give false images of crystalline-like structures in the  
309 background. After resuspension in buffer, cells were adhered onto poly-L-lysine-coated glass

310 coverslips and subsequently fixed with a solution of 2.5% glutaraldehyde in 0.05M cacodylate  
311 buffer. Samples were postfixed for 10 min in 1.5% OsO<sub>4</sub>, dehydrated in ethanol, and critical  
312 point dried with liquid CO<sub>2</sub>. The cells were then coated with technics hummer V coater and  
313 observed under a Zeiss 540 scanning electron microscope.

314 TEM: Similar to SEM, prior to fixation, control and treated cell pellets, that included primarily  
315 trophozoites or cysts depending on the treatment, were rinsed in 10% phosphate buffer solution,  
316 and centrifuged again. After resuspension in buffer, cells were adhered onto poly-L-lysine-  
317 coated glass coverslips and subsequently fixed in a solution of 2.5% glutaraldehyde in 0.05M  
318 cacodylate buffer. After fixation, the cells were post-fixed with 1% (wt/vol) OsO<sub>4</sub>, dehydrated  
319 with ethanol and acetone and embedded in epoxy resin. Ultrathin sections (1 micron) were  
320 contrast stained with uranyl acetate and lead acetate and observed under a Hitachi H-8100  
321 Transmission Electron Microscope fitted with AMT side mount digital camera.

322 *2.9. Induction of aromatic sterol synthesis.* Following the protocol of Korn [30] enabling the  
323 rapid induction of aromatase activity through cell disruption coupled to osmotic stress, control  
324 amoeba cell pellets harboring approximate  $1 \times 10^7$  cells/ml composed mostly of trophozoites  
325 (90%) were equilibrated for 20 min at zero degrees in 0.002 M CaCl<sub>2</sub> -0.001 M Tris buffer (pH  
326 7.0) and homogenized with three gentle strokes of a Douce homogenizer. Samples of 20 ml were  
327 incubated at 18 degrees for 6 h. At the end of the incubations, the lipids extracted with  
328 chloroform-methanol (2:1. v/v). The solvent was evaporated and the resulting organic layer  
329 analyzed by GC-MS/HPLC-UV or in separate study, preparative scale studies were carried out to  
330 isolate the major sterol products for <sup>1</sup>HNMR.

331 *2.10. Determination of AcCYP51 substrate affinity and product outcome*

332 The expression of pCWori<sup>+</sup>:AcCYP51 construct in *E. coli* has been described previously [32].  
333 Cytochrome P450 concentration, determined by reduced carbon monoxide difference spectra,  
334 and ligand binding studies [6, 38]. The dissociation constant of the enzyme-ligand complex ( $K_d$ )  
335 for each sterol or azole was determined by non-linear regression (Levenberg-Marquardt  
336 algorithm) using a rearrangement of the Morrison equation for tight ligand binding and the  
337 Michaelis-Menten equation when ligand binding was no longer tight [38]. Stock 2.5 mM sterol  
338 solutions were prepared in 40% (w/v) of 2-hydroxypropyl- $\beta$ -cyclodextrin (HPCD). All spectral

339 determinations were determined in triplicate. Curve-fitting of ligand binding data were  
340 performed using the computer program ProFit 6.1.12 (QuantumSoft, Zurich, Switzerland).  
341 Spectral determinations were made using quartz semi-micro cuvettes with a Hitachi-U 3310  
342 UV/Vis spectrometer (San Jose, CA). CYP51 enzyme activity from 10 min incubation was  
343 determined in triplicate using a CYP51 reconstitution assay system (0.5 ml final volume)  
344 composed of 1.14  $\mu\text{M}$  AcCYP51, 2.81  $\mu\text{M}$  *Aspergillus fumigatus* (AfCPR1-Q4WM67)  
345 cytochrome P450 reductase, 50 mM sterol substrate, 50 mM dilauryl phosphatidylcholine, 4%  
346 HPCD, 0.4 mg ml<sup>-1</sup> isocitrate dehydrogenase, 25 mM trisodium isocitrate, 50 mM NaCl, 5 mM  
347 MgCl<sub>2</sub> and 40 mM MOPS (pH, 7.2). In a preliminary study to establish approximate  $K_m$  and  $K_{cat}$   
348 kinetic constants for obtusifoliol against pure *Ac* C14-demethylase, reactions were carried out at  
349 37 °C with 1.14  $\mu\text{M}$  recombinant CYP51 and 2.74  $\mu\text{M}$  *Homo sapiens* CPR (as redox partner) at  
350 sterol concentrations of 6.25, 12.5, 25, 50, 75 and 100  $\mu\text{M}$  for 20 min. In a separate set of  
351 experiments, the  $k_{cat}$  for AcCYP51 against AfCPR1 was determined under assay conditions  
352 performed with the *Hs*CPR redox partner. Because the turnover number for obtusifoliol was  
353 distinctly low against *Hs*CPR redox partner we chose to evaluate sterol structure-activity against  
354 the redox partner of AfCPR. Enzyme-generated products were recovered by methanolic KOH  
355 saponification followed by extraction with 2 x 3 ml n-hexane, and then evaporation to dryness  
356 using a vacuum centrifuge. Product outcome was determined by GC-MS analysis of the free  
357 sterol. Competition experiments to establish IC<sub>50</sub> of azole against obtusifoliol were carried with  
358 the AcCYP51 and redox partner *Hs*CPR.

### 359 2.11. *AcSMT* Inhibition studies

360 Enzymatic assay conditions with soluble (cloned) *Ac*24-SMT or *Ac*28-SMT enzyme preparation  
361 and inhibition constant (IC<sub>50</sub>) determination against natural substrate and the 25-azacycloartanol  
362 inhibitor were essentially as described in the previous report [33]. Briefly, IC<sub>50</sub> values were  
363 determined from a dose-response curve against variable inhibitor concentrations in the range 0  
364 nM, 3.9 nM to 1  $\mu\text{M}$  in the presence of fixed-saturation- concentration of sterol acceptor (100  
365  $\mu\text{M}$ ) and coenzyme (150  $\mu\text{M}$ ). Assays were performed in triplicate with less than 10% deviation.  
366 IC<sub>50</sub> values were determined by standard graphical procedures for which computer-assisted  
367 linear regression analysis afforded correlation coefficients greater than 0.95 in a cases.  
368 Conversion of IC<sub>50</sub> value to  $K_i$  as dissociation constant, based on the experimentally deduced

369 kinetic properties of cycloartenol (24-SMT) or 24(28)-methylene lophenol (28-SMT) and 25-  
370 azacyclartanol was accomplished using the Cheng-Prusoff equation [38].

### 371 2.12. *GL7* growth

372 Sterol structure-membrane response effects were carried out using the *Saccharomyces*  
373 *cerevisiae* strain *GL7* with a defective 2,3-oxidosqualene to lanosterol synthase (*LAS*)  
374 auxotrophic for ergosterol, its natural membrane insert [8, 39]. *GL7* was cultured on 5 mg/l and  
375 Tween 80 (15 ml/l) in yeast-peptone-dextrose medium for 72 h affording growth arrest typical of  
376 wild-type yeast of  $1 \times 10^8$  cells/ml [8].

377

378

379

380

381

382

383

384

385

386

387

388

389

390

391

## 392 RESULTS

### 393 *3.1 Development of novel steroidogenesis patterns with growth and differentiation.*

394 A single cohort of viable cysts cultured on optimal growth conditions linked to extrinsic cues of  
395 salt stress or a decrease in carbon sources [23, 24] was used to observe excystment to replicative  
396 senescence-death and any associated sterol patterning. The initial experiments to observe  
397 differentiation included inoculum obtained from cysts determined to possess exclusively  $\Delta^5$ -  
398 sterols - brassicasterol and poriferasterol. Trophozoite proliferation, from  $10^4$  resting cysts/ml,  
399 followed a logarithmic course with a doubling time of 2.8 h. There seemed to be a slight  
400 induction period related to excystment phase of approximate 8-12 h yielding trophozoites.  
401 Amoeba cell proliferation reached growth arrest at approximately 3 days affording a cell density  
402 140 thousand cells/ml (Fig. 2, Panel A). As the amoeba continued in stationary phase, they began  
403 to progressively convert to encysted cells of mixed population of live and dead. The total cell  
404 number decreased with culture age as did the fresh weight of cultures by roughly a factor 10 at  
405 day 7 (Fig. 2, Panel B-inset). Continued incubation of the encysted cells for a month led to dead  
406 cells by trypan blue staining and to further decrease in the number of encysted cells by another  
407 factor of ten to about  $10^4$ /ml cysts remaining. Because some media preparations for amoeba  
408 growth include fetal bovine serum (FBS), which we determined contains  $10\mu\text{M}$  cholesterol, we  
409 added FBS as described in the American Type Culture Collection growth media or added  $10\mu\text{M}$   
410 cholesterol in DMSO to our growth media. In either case, the cholesterol supplement had only a  
411 minor stimulation effect on trophozoite growth.

412 To assess the conservation or change in sterol composition associated with differentiation, cells  
413 were harvested at 6 different stages in the excystment-trophozoite-encystment cycle at days 1, 2,  
414 3, 4, 7 and 1 month post-inoculation. The analysis demonstrated developmental changes in cell  
415 morphology and viability were accompanied by remarkable changes in steroidogenesis and  
416 metabolism. First, in what may be considered the amoeba growth phase, in the early logarithmic  
417 phase of growth in days 1 to 1.5 the  $\text{C}_{30}$  and  $\text{C}_{31}$ -cyclopropyl sterols -cycloartenol and 24(28)-  
418 methylene cycloartanol accumulate (Fig 2 and Suppl. Fig. 1), followed in logarithmic growth in  
419 days 2 to 3/3.5 by a shift to  $\Delta^{5,7}$ - $\text{C}_{28}$ - and  $\text{C}_{29}$ -sterol end product formation in approximate 5 to 7  
420 ratio (Fig. 2, Panel B and Suppl. Fig. 2).

421 At day 4 where the total cell number was similar to that at day 3, there was a mixed population  
422 of trophozoite and cysts and the sterol composition of the pelleted cells was a mixture of  
423 ergosterol, 7-dehydroporiferasterol, brassicasterol and poriferasterol roughly in a 50:50 ratio of  
424  $\Delta^{5,7}$  to  $\Delta^5$ -sterols. At day 7, most trophozoites had encysted (90% of total cells). The fresh weight  
425 of the cell pellet had decreased by a factor of 3 and the sterol composition of the encysted cells  
426 had reverted back to that of inoculum of  $\Delta^5$ - C<sub>29</sub>-sterol (90% of total sterol). (Figure 2, Panel B  
427 inset). At one-month incubation, after the remaining encysted cells had opportunity to excyst and  
428 proceed to trophozoite and then encyst again in cyclic fashion using up the carbon sources, most  
429 encysted cells were dead and contained predominantly C<sub>28</sub>- and C<sub>29</sub>- 6-methyl aromatic sterols,  
430 which we refer to as amebasterol-1 and amebasterol-2, respectively. These sterols were  
431 previously observed by Korn and Rohmer in *Acanthamoeba* as minor compounds (trace to 5%  
432 total sterol) [28-30, 40] from growth arrested cultures. We confirmed the structure of the major  
433 Ac sterols, as well as that of brassicasterol which is a newly characterized Ac sterol, through an  
434 examination of their chromatographic and spectral properties reported in Figure 3 (Suppl. Table  
435 1 for <sup>1</sup>HNMR analysis).

436 With this knowledge, the morphology and ultrastructure characteristics of trophozoites and  
437 encysted cells obtained from control (and subsequently treated cells) were determined. In light  
438 microscopy, inoculum cells generated by Method 2 against SDS (Materials and Methods) were  
439 found to possess the double-wall feature, and in transmission electron microscopy the  
440 encystment was evidenced in ultrastructure showing a nucleolus with a dense droplet in the cyst  
441 center, dense cytoplasm packed with lipid droplets, spherical mitochondria (M) and  
442 autolysosomes (A) that appear as large basophilic granules. Our observations, in agreement with  
443 Bowers and Korn [24], showed the mean diameter of rounded amoeboid cells were  
444 approximately  $26.5 \pm 0.17 \mu$  whereas the mean cytoplasmic diameter of cysts was  $16.2 \pm 0.13 \mu$ .  
445 The decrease in surface area during encystment of a cell of median diameter was more than 65%  
446 while the decrease in median cell volume was approximately 80%, suggesting significant loss of  
447 cell membrane from amoeba to true cyst. The sterol content in trophozoite and true cyst was 12  
448 pg/cell and 4 pg/cell, respectively. Thus, there is both a distinct loss in total sterol and a marked  
449 metabolism of preformed  $\Delta^{5,7}$ -sterol as trophozoite converts into the true cyst form. These sterol  
450 modifications correlate to the different membrane requirements of non-encysted and encysted  
451 cells capable of excystment (Figure 2). Once true cysts differentiate into trophozoites, the



452 resulting amoeba, observed to synthesize ergosterol and 7-dehydroporiferasterol, were examined  
453 by light and electron microscopy. These non-encysted amoebae were shown to contain typical  
454 cytoplasmic organelles, such as a nucleus with a prominent nucleolus, an abundant rough  
455 endoplasmic reticulum, mitochondria, vacuoles and lipid droplets and showed surface  
456 protrusions -acanthopodia, durable double wall of smooth ectocyst and a round endocyst (Fig. 2,  
457 Panel C).

458 *3.2. Medium-replacement induced-encystment can lead to distinct cell types of characteristic*  
459 *sterol compositions.*

460 To determine whether the unusual  $\Delta^5$ -sterol and 6-methyl aromatic sterol profiles observed in the  
461 stationary phase growth were associated with distinct cyst populations, we initiated encystment  
462 by Method 2. The salt stressed trophozoite cultures spontaneously encysted yielding some cell  
463 debris. GC-MS analysis of the pellet extract revealed 21 sterols (Suppl. Fig. 2, Panel E and Table  
464 1) which is the most complex sterol composition reported for not only the amoeba but for  
465 protozoa generally. Many of these sterols represent co-metabolites and by-products. Of interest  
466 was the experimentally induced encystment of amoeba yielded a sterol mixture of  $\Delta^{5,7}$ -sterols,  
467  $\Delta^5$ -sterols and 6-methyl aromatic sterols. Notably, no significant trophozoites were detected  
468 microscopically, yet there is a significant amount of ergosterol and 7-dehydroporiferasterol in the  
469 sterol mixture suggesting that a subset of encysted cells could possess  $\Delta^{5,7}$ -sterols. As the  
470 encysted cells were processed further through SDS-treatment, the cells that remain contain  
471 predominantly brassicasterol and poriferasterol by GC-MS analysis (Supple Fig. 2, Panel F);  
472 these cells are viable and can excyst completely to trophozoites in enriched medium in 12 h. We  
473 surmise the salt step can create mixed populations of encysted cells; one population is composed  
474 of fragile double walls and membranes composed of  $\Delta^{5,7}$ -sterols or aromatic sterols and a second  
475 population is composed of resistant double-wall structures and membranes composed of  $\Delta^5$ -  
476 sterols.

477 A crucial observation made by the Korn group to prepare an abundance of 6-methyl aromatic  
478 sterols of the phenanthrene skeleton was to generate a cell-free system of Ac in high salt solution  
479 yielding a microsomal (membranes) subcellular fraction. Under these conditions, the ergosterol  
480 and 7-dehydroporiferasterol rapidly convert in stoichiometric fashion to amebasterol-1 and  
481 amebasterol-2; the aromatic compounds remain membrane-bound [30]. The relevance of the

482 Korn study is to show both that the phenanthrene steroids can be easily obtained in amounts  
483 necessary for structure determination and that these aromatic compounds can associate with the  
484 endoplasmic-plasma-membrane fraction of microsomes in intact cells. Notably, this approach  
485 used by Rohmer on the related *Acanthamoeba* species-polyphaga yielded sufficient compound to  
486 be characterized by  $^{13}\text{C}/^1\text{H}$ -NMR to prove the structure and stereochemistry of the metabolites as  
487 new class of steroids [31]. We repeated these studies and observed *Ac* homogenates generate 6-  
488 methyl aromatic sterols from  $\Delta^{5,7}$ -sterols in amounts reported by Korn over the 6 h incubation  
489 period. The 6-methyl aromatic sterols can remain stable for at least 2 months (Suppl. Figure 2,  
490 Panels G and H).

### 491 3.3. Catalytic competence of *AcCYP51* relative to *Ac24-SMT* and *Ac28-SMT*.

492 The functional expression in *E. coli* of pC *Wori*<sup>+</sup>:*AcCYP51* construct and wild-type cDNA of 24-  
493 SMT and 28-SMT have been described previously [32, 33]. To elucidate the diversity of  
494 substrate preference that could influence the order of intermediates in C<sub>28</sub>- and C<sub>29</sub>- sterol  
495 synthesis, eleven 14-methyl sterols were evaluated for substrate recognition by *AcCYP51* (Table  
496 2, Suppl. Fig. 3 to 6). When the redox partner for *AcCYP51* activity was *AfCPR1* the rate of  
497 formation of product was greater by a factor of 10 compared to using the *HsCPR* redox partner  
498 affording approximately  $7.6 \pm 0.05 \text{ min}^{-1}$ . Consequently, we used the *AfCPR1* redox partner to  
499 determine structure-activity.

500 After incubation in the usual way, no metabolism occurred with cycloartenol, whereas  
501 obtusifoliol was fully metabolized by *AcCYP51* under the same conditions as evidenced in GC-  
502 MS analysis showing the  $\Delta^{8,14}$ -product in 95% yield (Suppl. Fig. 4). Because the rate of product  
503 formation against the *AfCPR1* partner was much higher than when using the *HsCPR* redox  
504 partner, we could now detect some small conversion of cycloeucalenol. This was evident in two  
505 ways; in catalytic assay to establish competence afforded a rate of  $0.04 \pm 0.01 \text{ min}^{-1}$  and in GC-  
506 MS analysis showing a new cyclosteroid product ( $\text{M}^+410$ , ~1% yield,) that contained the  $\Delta^8$ -  
507 structure (Suppl. Fig. 4, structure **24** in Table 1). While doubtful the new metabolite converts to  
508  $\Delta^{5,7}$ -sterol under physiological conditions, it does shows mechanistically that the  $\Delta^8$ -bond is not  
509 essential for CYP51 activity. In contrast, a  $\Delta^8$ -bond in the CYP51 substrate is required in plant  
510 and animal sterol biosynthesis [41-43]. Except for cycloeucalenol as substrate, there was general  
511 agreement between affinity and catalytic competence determined by the sterol difference spectra

512 and binding constant ( $K_d$ ) and efficiency for substrate to be converted to 14-desmethyl product  
513 ( $k_{cat}$ ). Those substrates having a 9,19-cyclopropyl group, typical of intermediates in the plant  
514 sterol biosynthesis pathway, poorly bind to the enzyme (cycloeucaleanol) or not at all  
515 (cycloartenol and 24(28)-methylene cycloartanol). Structural isomers of the cyclopropyl sterol  
516 that possess a  $\Delta^7$ -bond do not bind while those that possess a  $\Delta^8$ -bond bind well with obtusifoliol  
517 (Suppl. Fig 3- **10**) the apparent favored substrate for AcCYP51. While not readily evident from  
518 the affinity constant ( $K_d$ ), but apparent from the rate data ( $k_{cat}$ ) through comparison of pairs of  
519 substrates that differ in side chain construction for a  $\Delta^{24(28)}$ -group of lanosterol (Suppl. Fig. 3 -  
520 **33**) versus eburicol (Suppl. Fig. 3 - **32**), obtusifoliol (Suppl. Fig. 3- **10**) versus 31-norlanosterol  
521 (Suppl. Fig. 3- **37**), it appears that AcCYP51 prefers a substrate that possesses the 24(28)-bond  
522 (Table 2) consistent with its phylogenetic association to land plant enzymes [6] and provides  
523 rationale for the biosynthetic ordering of intermediates.

524 Thus, in good agreement with results of the titration experiments and catalytic parameters of the  
525 AcCYP51 the enzyme clearly prefers obtusifoliol (Table 2) yielding an optimal rate for C14-  
526 demethylation of  $7.6 \text{ min}^{-1}$ . The value is close to the  $V_{max}$  reported for kinetoplastid protozoan  
527 and land plant CYP51 and is approximately 6 fold lower than those for the fungal and human  
528 isoforms [6]. On the basis of the previously determined catalytic competence of cloned AcSMTs  
529 (referenced in Table 2), it has been shown cycloartenol [ $k_{cat} 1.5 \text{ min}^{-1}/K_m 44 \mu\text{M}$ ] is the favored  
530 substrate for 24-SMT and the enzyme generated product is 24(28)-methylene cycloartanol while  
531 24(28)-methylene lophenol [ $k_{cat} 0.8 \text{ min}^{-1}/K_m 25 \mu\text{M}$ ] is the favored substrate for 28-SMT which  
532 converts to multiple 24-ethyl sterol  $\Delta^{25(27)}$  - and  $\Delta^{24(28)}$  - products [33]. Comparative analysis of  
533 the sterol C14-demethylase and C24-methylase specificity reveal neither of the AcSMT  
534 recognizes obtusifoliol as substrate and that AcCYP51 fails to productively accept either of the  
535 AcSMT favored substrate.

536 *3.4. Identification of a new sterol biosynthesis in protozoa; evidence for separate intermediates*  
537 *to C<sub>28</sub> - and C<sub>29</sub>-sterols.*

538 There is no clear information about the C<sub>29</sub>-sterol synthesis pathway. In the first round of  
539 trophozoite sterol analyses, we identified 15 neutral sterols (other than the novel aromatic  
540 sterols) from the MgCl<sub>2</sub> treated cultures (compounds **1, 2, 3, 4, 5, 6, 7, 8, 9, 11, 12, 13, 17, 18**  
541 and **20**, Suppl. Fig. 2 and 3) and from logarithmic phase cultures 4 more sterols were detected

542 (Suppl. Fig 1 **16**, **19**, **21** and **27** and illustrated in Suppl. Fig. 3) while additional sterols were  
543 obtained from treated cultures corresponding to many of the compounds previously isolated from  
544 *Acanthamoeba polyphaga*, including cycloartenol, 24(28)-methylene cycloartanol, obtusifoliol,  
545 24 $\beta$ -ethyl cholesterol and 24 $\beta$ -methyl cholesterol [28, 29]. Our chemical identification of Ac  
546 cycloartenol by GC-MS against a standard available to us and of parkeol synthesized from  
547 cycloartenol by acid-induced rearrangement of the cyclopropane ring to the 9(11)-structure [44]  
548 agrees with the careful biochemical and enzymological studies of Rohmer showing as well that  
549 cycloartenol is the sole product of 2,3-oxidosqualene cyclization to protosterol in *A. polyphaga*  
550 and 9(11)-metabolites occur as byproducts in trace amounts [28, 29]. Our observations combined  
551 with that of Rohmer for cycloartenol rather than lanosterol as the true protosterol for  
552 *Acanthamoeba* species is supported by Ac genome mining for sterolic enzymes where a single  
553 2,3-oxidosqualene to protosterol synthase (cyclase) is detected corresponding to the cycloartenol  
554 synthase (*CAS1*). Recent phylogenetic studies have shown that *CAS1* can be distinguished from  
555 the gene for lanosterol synthase (*LAS1*) through a signature peptide sequence with a conserved  
556 residue at amino acid position-442 (Ac numbering system) for isoleucine rather than valine  
557 characteristic of the lanosterol synthase (*LAS1*), as shown in supplemental Figure 7 [13, 45 and  
558 references cited therein]. Testing effects of substitution of the conserved residues in and around  
559 position 442 (Ac numbering) on *CAS1* and *LAS1* have led to the notion that high conservation of  
560 the amino acid composition in these regions represents an important structural basis for  
561 evolutionary conservation of protosterol formation [13], and indicate that cycloartenol evolved  
562 before lanosterol.

563 For elucidation of new biochemical transformations and biosynthetic pathways mass spectra of  
564 sterols identified in GC-MS analysis are extremely powerful tools in providing information about  
565 multiple structural features of the molecule. In many cases authentic compounds are recorded in  
566 the recently released NIST library of chemical standards. A molecular ion is normally observed  
567 in the mass spectrum of free sterol which is reason we have studied this sterol form in GC-MS  
568 analysis. It is preferable to consider fragmentation patterns and subtleties in ion intensity  
569 associated with the ring and side chain in formulating sterol structure [46]. For those that rely on  
570 the NIST library to assign structure to sterols caution should be exercised since partial  
571 information is obtained from observation of molecular ion and base peak of target sterol as  
572 match indicators and thus can lead to erroneous structure assignments for several key compounds

573 as reported in reference 34. Importantly, many reference sterols that occur naturally are not  
574 entered into the NIST library. For example, the aromatic sterols identified in this study, e.g.,  
575 amebasterol-1 of  $M^+$  394 amu, is matched to 9-methyl anthrasteroid (anthraergostatraenol) in the  
576 NIST library with 81.1% match of 86.7 % probability. This seemingly excellent match in the  
577 database generates an incorrect structure for the Ac compound while the correct structure has yet  
578 to be deposited into the NIST library. Indeed, Rohmer proved through NMR studies, and  
579 confirmed here, the structure of this Ac metabolite as the phenanthrene skeleton harboring an  
580 aromatic B-ring with the C19 methyl rearranged to the C6-position [31]. Another relevant  
581 example for potential inaccuracy in structure determination as it relates to Ac sterol biosynthesis  
582 pathways comes from the supposed mass spectrum match of ergosterol which has the  $\Delta^{5,7,22}$  -  
583 triene system. Its  $\Delta^{25(27)}$  -ergostene isomer, like that of its  $\Delta^{24(28)}$  - and  $\Delta^{24(25)}$  -ergostene isomers,  
584 have identical mass spectra and one of more of these isomers can co-elute with ergosterol in GC  
585 unless appropriate chromatographic conditions are met [19, 46]. Referencing the NIST library is  
586 further limited in the identification of the set of B-ring structural isomers of  $\Delta^8$  versus  $\Delta^7$ -  
587 ergostenes, for the set of conjugated B/C-ring dienes of  $\Delta^{5,7(8)}$ ,  $\Delta^{8,14(15)}$ ,  $\Delta^{5,8(9)}$ ,  $\Delta^{6,8(14)}$  -ergostene  
588 isomers and for the C24-alkyl epimers (for example) poriferasterol (24 $\beta$ -ethyl) and stigmasterol  
589 (24 $\alpha$ -ethyl) [46-49]; in the usual practice, identification of the individual isomers is confirmed  
590 through a comparison of chromatographic and spectral constants of the unknown as the free  
591 alcohol or as a C3-derivatized compound to assist in chromatographic resolution against  
592 equivalent data obtained on authentic standards or for determination of stereochemistry at C24  
593 through NMR of the pure compound or as necessary to synthesize the applicable standard [48].

594 Previously isolated sterols from *Acanthamoeba* are variably positioned as intermediates in  
595 biosynthetic schemes for ergosterol and 7-dehydroporiferasterol synthesis, including a  
596 hypothetical terminal step whereby  $\Delta^5$ - C<sub>29</sub>-monoene sterols (24-ethyl cholesterol), formed from  
597  $\Delta^{5,7}$ -sterol, convert to final  $\Delta^{5,22}$ -diene sterol, as can occur in land plants. Curiously, the  $\Delta^{25(27)}$  -  
598 C<sub>29</sub>-sterols that we observed in trace amounts in *A. castellanii* were detected also in trace  
599 amounts in *A. polyphaga* and *A. culbertsoni* by research groups with expertise in natural product  
600 characterizations [28, 50]. However, the earlier investigators failed to consider the biosynthetic  
601 importance of  $\Delta^{25(27)}$  -sterols to ergosterol and 7-dehydroporiferasterol synthesis, relegating them  
602 to by-products in the sterol metabolome. The accumulation of ergost-5-enol and poriferast-5-  
603 enol [structures 4 and 14 in Suppl. Fig. 3] which arise from the salt treatments is problematic and

604 may not relate to their biosynthetic intermediate role in  $\Delta^{5,7}$ -sterol formation of ergosterol and 7-  
605 dehydroporiferasterol as proposed [28]. Rather, these sterols may be considered metabolically  
606 inert end products formed along with brassicasterol and poriferasterol from a  $\Delta^7$ -reductase of  
607 broad substrate specificity during encystment and not from trophozoite growth (Fig. 6). As our  
608 studies suggest, the  $\Delta^7$ -reductase appears only to be active during the encystment process.

609 Incubation of [*methyl*- $^2\text{H}_3$ ]methionine with trophozoites revealed growth arrested cultures  
610 possessed three major isotopically labeled sterols corresponding to ergosterol, poriferasterol and  
611 7-dehydroporiferasterol; for ergosterol the mass spectrum showed the dideuterated species ( $\text{M}^+$   
612  $396 \rightarrow \text{M}^+ 398$ ) while the mass spectrum of 7- dehydroporiferasterol showed the pentadeuterated  
613 species ( $\text{M}^+ 410 \rightarrow \text{M}^+ 415$ ) and the mass spectrum of poriferasterol showed the  
614 pentadeteuterated species ( $\text{M}^+ 412 \rightarrow \text{M}^+ 417$ ) (Figure 2, Panels E and F). The fragment  
615 containing the high end molecular cluster at  $m/z$  396 for ergosterol and  $m/z$  410 for 7-  
616 dehydroporiferasterol derived from the methyl cation on SAM was shifted by 2 Da or by 5 Da,  
617 respectively, in the mass spectra of the labeled sterol (Suppl. Fig. 8) These labeling results show  
618 a mixed biosynthetic pathway in which ergosterol is formed by an  $\Delta^{24(28)}$  - sterol methylation  
619 pathway similar to land plants which incorporate 2 D- $^2\text{H}_3$ -SAM atoms at  $\text{C}_{28}$  while the 7-  
620 dehydroporiferasterol and poriferasterol sterol  $\text{C}_{29}$ -methylation pathways are similar to the  $\Delta^{25(27)}$   
621  $-\text{C}_{29}$ -sterol methylation pathway in green algae which incorporate 5-D  $^2\text{H}_3$ -SAM atoms into the  
622  $\text{C}_{29}$ -sterol [19, 45]. In contrast, land plant  $\text{C}_{29}$ -sterol biosynthesis 4D  $^2\text{H}_3$ -SAM atoms are  
623 incorporated into the 24-ethyl group consistent with the involvement of a  $\Delta^{24(28)}$  - $\text{C}_{29}$ -sterol  
624 intermediate [51]. The enzyme-catalyzed conversion of  $\Delta^{24(25)}$  -sterol substrate to  $\text{C}_{28}$ - and  $\text{C}_{29}$ -  
625 sterol products were considerably altered from the sterol profile of control. As shown (Figure 2,  
626 Panel B), the composition of the sterol mixtures obtained from cultures grown on normal and  
627 deuterium-labeled methionine showed that the proportion of  $\text{C}_{28}$ -sterol was markedly increased  
628 while the  $\text{C}_{29}$  sterols decreased in the cultures grown in the presence of [*methyl*- $^2\text{H}_3$ ]methionine.  
629 These labeling experiments reveal the operation of a pronounced deuterium isotope effect and  
630 indicates that the proton loss from a  $\text{C}_{28}$  intermediate (Figure 5, Panel A) is the rate-limiting step  
631 in formation of  $\text{C}_{29}$ -sterol products. Thus, in the presence of substrate 28-SMT affording  $\text{C}_{29}$ -  
632 sterols can in some circumstances significantly alter the course and equilibrium of metabolic  
633 sequences affecting the balance of  $\text{C}_{28}$  to  $\text{C}_{29}$ -sterols during growth and differentiation. For  $\text{C}_{29}$ -  
634 sterols there is switch to an alternate route utilizing  $\Delta^{25(27)}$ -intermediates in contrast to the

635 previously reported route of  $\Delta^{24(28)}$ -intermediates [28]. It should be remembered the cell pellet  
636 used for our sterol analysis was from a culture composed of two populations of cells—  
637 trophozoites that synthesize  $\Delta^{5,7}$ -sterols and encysted cells that contain  $\Delta^5$ -sterols. Given the  
638 differentiation processes discussed in section 3.1, it is more likely the poriferasterol is derived  
639 from the 7-dehydroporiferasterol associated with trophozoite to encysted cell formation. It is also  
640 notable the phytosterols synthesized in land plants possess side chain C24/methyl/ethyl  
641 structures that are  $\alpha$ -oriented while our  $^1\text{H}$ NMR analysis of the *A. castellanii* ergosterol and 7-  
642 dehydroporiferasterol indicated the C24-methyl/ethyl structures are  $\beta$ -oriented similar to the side  
643 chain structures of C<sub>28</sub>-and C<sub>29</sub>-sterols in the green alga *Chlamydomona reinhardtii* [19].

644 Conventional co-metabolite ordering in Ac sterol biosynthesis suggests the amoeba operates a  
645 land plant phytosterol biosynthesis pathway via the cycloartenol to 24(28)-  
646 methylenecycloartanol  $\Delta^{24(28)}$ -pathway to C<sub>28</sub>- and C<sub>29</sub>-sterol final products. However, through a  
647 comparison of the Ac genomic database with land plant (*Arabidopsis*) genomic database (and for  
648 aromatase the human genome database) together with our chemical analysis of trophozoites and  
649 encysted cells, we reconstructed the cycloartenol to 6-methyl aromatic sterol biosynthetic  
650 pathways, taking into account phylogenetic differences in the sterol methylation of  $\Delta^{25(27)}$  –  
651 (green algae) and  $\Delta^{24(28)}$ -olefin (land plant) routes and in the formation of  $\Delta^{5,7}$ -sterols versus  $\Delta^5$ -  
652 sterols (Fig. 6). The reconstruction of the *A. castellanii* sterol pathway underscores the  
653 metabolic divergence of amoeba and recurrent evolution. The results show: (i) completion to a  
654  $\Delta^5$ -monoene sterol atypical of green algae, (ii) selective sterol methylation for the 24 $\beta$ -  
655 orientation typical of green algae (iii) *in vitro* AcSMT assays show obtusifoliol is not a substrate  
656 and that  $\Delta^{25(27)}$ -sterol is a product of the enzyme catalyzed reaction consistent with ordering of  
657 intermediates based on biosynthetic reasonableness, and (iv)  $^2\text{H}$ -methinone fed to Ac show the  
658 C<sub>28</sub> - and C<sub>29</sub>- sterol products are formed by separate  $\Delta^{24(28)}$  – C24-methylene and  $\Delta^{25(27)}$  -olefin  
659 C24-ethyl intermediates, respectively, and that any  $\Delta^{24(28)}$  -24-ethyl sterols formed enzymatically  
660 are redundant not incorporated into 7-dehydroporiferasterol under physiological conditions.

### 661 3.5. Dependence of inhibitor effect on the physiological state of the amoeba cells

662 The primary mechanism of the azole and steroidal inhibitor effect- inhibition of ergosterol  
663 biosynthesis in amoeba cells- has as a prerequisite an active cellular metabolism for the  
664 biosynthetic renewal of ergosterol with proliferation and growth. It is understandable that

665 dormant cysts could only be affected at high concentrations of these drugs (>100  $\mu$ M), if at all.  
666 However, unclear is the extent to which the encysted cell can alter its sterol profile in response to  
667 an ergosterol biosynthesis inhibitor. The aza analog of the C25-carbocation intermediate of the  
668 C24-methylation reaction, a steroidal inhibitor, against *Ac24SMT* and *Ac28-SMT* and the tight  
669 binding inhibitor voriconazole against *AcCYP51* were utilized to determine the relative  
670 importance of active site interactions of select sterol biosynthesis enzymes responsive to these  
671 drugs *in vitro* as well as in cell-based studies

672 The effect of azole and 25-azacycloartanol (Fig. 7, Panel A) on rapidly proliferating trophozoites  
673 was much the same—both compounds prevented amoeba growth at low inhibitor concentrations  
674 of  $IC_{50}$  values 390 nM and 25 nM, respectively and MAC values between 1-3  $\mu$ M (Fig. 7, Panel  
675 B). Sterol analysis of mostly encysted cells revealed mark changes to the  $C_{28}$ - and  $C_{29}$ - sterol  
676 balance associated with encystment (Suppl. Fig. 2, Panel C and Suppl. Fig. 9) and the total sterol  
677 content was less than in trophozoite by approximately 50% on per cell or pellet basis. Although  
678 steroidal inhibitor treatment resulted in reduced  $C_{29}$ -sterol levels, showing disruption in substrate  
679 pools, there was not much accumulation of intermediates cycloartenol or obtusifoliol, suggesting  
680 a down-regulation of *de novo* sterol synthesis as trophozoite converts to encysted cell as reported  
681 elsewhere [35]. In neither treatment was there significant accumulation of 6-methyl aromatic  
682 sterol. However, after the treated cells were incubated for another 8 days all the  $\Delta^{5,7}$ -sterol had  
683 converted to 6-methyl aromatic sterol accompanied by a ten- fold decline in fresh weight of the  
684 pellet. When the concentration of inhibitor is increased 10 to 50 fold, i.e., increasing stress, the  
685 resulting 48 cell pellet is composed exclusively of dead cells and the sterol profile consists  
686 mostly of 6-methyl aromatic sterol.

687 To determine whether FUdR, a DNA synthesis inhibitor [52] that should prevent ergosterol  
688 biosynthesis globally, had an effect on differentiation, spontaneous encystment was evaluated  
689 after the cultures containing inhibitor reached stationary phase of control. The resulting cells had  
690 a population of cysts equal to the parent trophozoite inoculum of approximately  $2-3 \times 10^5$   
691 cells/ml. Effectively all of these encysted cells (>95%) were alive according to trypan blue  
692 staining. The FUdR treated cells showed a significant increase in  $\Delta^5$ -sterol of brassicasterol and  
693 poriferasterol (40 % total sterol) which associates with true cyst formation (Suppl. Fig. 10). In  
694 contrast, for treatments with voriconazole or 25-azacycloartanol the number of cells at 48 h was



695 reduced by a factor of 10 to  $2-3 \times 10^4$  cells/ml, most were dead by trypan blue staining (Fig. 7,  
696 Panel B) and they (encysted cells) possessed mostly ergosterol and 7-dehydroporiferasterol  
697 (Suppl. Fig. 9) with no accompanying 6-methyl aromatic sterol.

698 Time-killing experiments were carried out by the addition of inhibitor at approximate MAC  
699 levels to the culture medium for 48 incubations. Figure 7 (Panel C) shows that medium  
700 inoculated with a population of  $1 \times 10^5$  cells/ml trophozoites (90%) affords continued  
701 trophozoite proliferation, without significant encystment (data not shown), to a stationary phase  
702 population of  $1 \times 10^6$  cell/ml. Alternatively, in the presence of the test inhibitors, at about the  
703 MAC, the trophozoite population drops to zero. This stressing of amoeba stimulates trophozoite  
704 to encyst, which as inhibitor pressure is maintained yields a decrease in the total number of  
705 encysted cells from approximate  $3 \times 10^4$  encysted cells/ml at 12 h to an approximate  $5 \times 10^2$  to  $5$   
706  $\times 10^3$  cells/ml at 48 h growth. Trypan blue staining of the encysted cells revealed two dominant  
707 populations characterized by those that are viable or non-viable and dead. When the 48 h treated  
708 pellets were transferred to fresh medium and incubated for a week, 25-azacycloartanol  
709 treatments showed no growth while from the voriconazole treatment a few thousand trophozoites  
710 were evident, suggesting the predominant population of encysted cells viewed as dead by trypan  
711 blue staining were indeed dead in terms of excystment.

712 Because the clumped cells were in much greater density in treated cells than in control, it was  
713 straightforward to examine them by scanning electron microscopy (SEM) and transmission  
714 electron microscopy (TEM). Thus, SEM and TEM images of 25-azacycloartanol-generated cysts  
715 (VOR looked much the same) from the 48 h harvest were virtually the same as those of control  
716 cysts originating in T-flasks showing one or more flaccid cells clumped together with rounded  
717 cells (cf. Figure 2, Panel C). Fine structure of the treated cells also showed a deformation in cell  
718 wall associated with an aberrant thickening or partially formed ectocyst and endocyst, and the  
719 cell interior looked severely damaged with (i) formation of blebby structures in the cell  
720 membrane, (ii) broken membrane structures and (iii) intense vacuolization and loss of  
721 mitochondria typically associated with autophagy-like structures in the center of the cell that  
722 contained undigested organelle.

723 To determine whether inhibitors designed to block two essential enzymes in the post-squalene  
724 segment of the ergosterol biosynthesis pathway are more potent in combination than when added

725 to the medium singly, we monitored the effects of combining subinhibitory concentrations of one  
726 drug against varied concentrations of the other drug on trophozoite multiplication. Complete  
727 eradication of the amoeba parasite is obtained when using the drugs in combination at  
728 concentrations as low as equal to their IC<sub>50</sub> values which in our studies for voriconazole was 140  
729 nM ± 10 nM compared to our previously reported 390 nm [32] and for 25-azacycloartanol is 25  
730 nM ± 2 nM (Fig. 7, Panel D). The number of dead cells at 48 h in the combination drug  
731 experiment of 25 nM 25-azacycloartanol (25 nM) and voriconazole (100 nM) was similar to the  
732 number of dead cells when the drugs were administered individually to the medium (Fig. 7,  
733 Panel B), and no trophozoites were detected after 5 days following resuspension of treated pellet  
734 into fresh medium. These results suggest that combined treatment of two or more rationally  
735 designed inhibitors at sub-MAC concentration can successfully interfere with sterol biosynthesis  
736 to prevent leakiness at the target enzyme and in so doing limits production of the downstream  
737 C<sub>28</sub>- and C<sub>29</sub>-sterols, supporting a role for AcCYP51 and AcSMTs in the control of metabolic flux  
738 through distinct intermediates.

### 739 *3.6 Excystment in response to inhibitor treatment.*

740 In a separate experiment the anti-amoeba effect of the drugs on excystment was determined with  
741 cysts derived from the SDS-treated process. Using MAC concentrations of the ergosterol  
742 biosynthesis inhibitors, all the resting cysts convert to trophozoites by 5 days, indicating that  
743 excystment is insensitive to these treatments. In similar fashion, the FUDR treated resting cells  
744 easily excysted into trophozoites by 3 days. During these experiments, increase numbers of  
745 empty cyst walls were evident in cell mixture, consistent with excystment.

### 746 *3.7. Enzymatic basis of action and selectivity.*

747 All the available experimental evidence indicates that AcCYP51 and 24-/28-AcSMT are the  
748 primary target of the medical azole and steroidal N-inhibitor, respectively, since we observed  
749 small accumulations of obtusifoliol and cycloartenol in the presence of voriconazole and  
750 24(*R,S*),25-epiminolanosterol [32, 33]. The target enzymes were characterized from cloned genes  
751 introduced into *E. coli* and solubilized for activity assay. In our earlier study, we observed that  
752 voriconazole is a specific and reversible inhibitor of AcCYP51 exhibiting an IC<sub>50</sub> of 390 nM and  
753 its MAC is approximately 3 μM [32, 33]. 25-Azacycloartanol tested as a true substrate analog

754 inhibitor is approximately as effective against 24-AcSMT and 28-AcSMT as voriconazole  
755 against AcCYP51. The inhibitor against trophozoite proliferation generates an  $IC_{50}$  of  $25 \text{ nM} \pm$   
756  $0.25 \text{ nM}$  and MAC of  $1 \text{ } \mu\text{M} \pm 0.05 \text{ } \mu\text{M}$  (data not shown) and against 24-SMT incubated with  
757 cycloartenol as substrate or 28-SMT incubated with 24(28)-methylene lophenol as substrate  
758 yields  $IC_{50}$  values of  $15 \text{ nm}$  ( $K_i = 13 \text{ nM}$ ) and  $22 \text{ nM}$  ( $K_i = 8 \text{ nM}$ ) (Suppl. Fig. 11). The measured  
759 inhibition of the AcCYP51 and SMT activities is quantitatively sufficient to account for the  
760 inhibition of ergosterol and 7-dehydroporifersterol biosynthesis in amoeba.

### 761 3.8. Effect of *Acanthamoeba* sterols on growth of GL7

762 To assess the structural specificity for sterols as membrane inserts directly, we used the yeast  
763 GL7 auxotrophic for sterol. Close interactions between sterol supplementation and the growth  
764 response was detected. Ergosterol supplementation to GL7 afforded growth arrest in 72 h  
765 affording approximate  $1 \times 10^8$  cells/ml, typical of wild-type yeast, while cultures without added  
766 ergosterol yielded a no growth-response, as reported previously (Fig. 8) [8, 39, 53]. Ergosterol  
767 was recovered in unchanged form from the cells at approximately 20 fg/cell. Microscopic  
768 examination showed the GL7 yeast at growth arrest revealed mostly single cells or those that  
769 were undergoing budding. Alternate sterol supplements fed to GL7, 7-dehydroporiferasterol,  
770 brassicasterol, poriferasterol reached a stationary phase of  $1 \times 10^8$  cells/ml similar to the  
771 ergosterol fed cells and each of the sterols was recovered from cells in unchanged form at 20  
772 fg/cell. Alternatively, cells fed the 6-methyl aromatic sterol supplement failed to proliferate by  
773 72 and microscopically many cells were clumped or dead by trypan blue staining typical of yeast  
774 cultured on a steroidal inhibitor [53]. Past interpretation using the GL7 system showing a no  
775 growth response following administration of nutritionally adequate amounts of sterol is the  
776 supplement failed to adequately fit the membrane structure [7, 8].

777

778

779

780

781

## 782 DISCUSSION

783 In spite of the therapeutic importance for an exacting sterol composition in parasitic protozoa  
784 [27], relatively little is known about the regulation and function of phytosterols in amoeba. This  
785 lack of information on metabolic controls is a serious impediment to the development of  
786 strategies for targeted inhibition of phyla-specific enzymes, such as the sterol C24-methylase,  
787 that can occur in the protozoan pathogen while absent from the human host. Previous functional  
788 and phylogenetic analysis of amoeba steroidogenesis has left the role and origins of C<sub>28</sub>- and C<sub>29</sub>-  
789 sterols somewhat opaque. In particular, while it seems clear the *Acanthamoeba* can synthesize  
790 ergosterol and 7-dehydroporiferasterol, it has been assumed there is one set of terminal  
791 compounds –  $\Delta^{5,7}$ -sterols - that act unaltered as membrane inserts and for the sterol biosynthetic  
792 genes to be descended from plants. However, the possibility for evolutionary accommodation of  
793 stage-specific differences in  $\Delta^5$ -,  $\Delta^{5,7}$ - and 6-methyl aromatic compounds in *Acanthamoeba* was  
794 indicated by GC-MS analysis of mixed populations of trophozoites and encysted cells, although  
795 it was ignored, leading to the view that  $\Delta^5$ - sterols are the precursor of  $\Delta^{5,7}$ -sterols, that the C24-  
796 methylation  $\Delta^{24(28)}$  -route typical of land plants yield intermediates for the synthesis of C<sub>28</sub>- and  
797 C<sub>29</sub>-sterols and for the sterolic enzymes to lack substrate specificity affording criss-crossing  
798 routes of major and minor biosynthesis pathways to final  $\Delta^{5,7}$ -sterol products [2, 29, 54].  
799 Subsequent co-metabolite and phylogenetic analysis based on an erroneous characterization of  
800 many of the reported amoeba sterols, incorrect bioinformatic analyses for identity of the 2,3-  
801 oxidosqualene cyclase as lanosterol synthase and failure to report a SMT2-type isoform required  
802 in the synthesis of 24-ethyl sterols [34] developed an enigmatic history for *Acanthamoeba*  
803 ergosterol biosynthesis pathway as originating with the fungi.

804 Here and in our previous paper [33] we provide evidence for the first time that indicates the  
805 sterol biosynthetic enzymes in *Acanthamoeba* were composed of catalytically constrained  
806 participants of strict substrate specificity, for sterol methylases to be responsible for generating  
807 distinct  $\Delta^{24(28)}$  - and  $\Delta^{25(27)}$  -olefin intermediates that convert to functional C<sub>28</sub>- and C<sub>29</sub>-sterol  
808 products of varied nucleus structures and that the conventional sterols typical of protozoa  
809 ergosterol and 7-dehydroporiferasterol can be replaced with the uncommon brassicasterol-  
810 poriferasterol and amebasterol-1 and amebasterol-2 steroidal pairs during the encystment phase  
811 of the amoeba life history. Because methylation patterns in large part determine product

812 outcome, subtle alterations in methyltransferase substrate selectivity have a profound impact on  
813 the balance of C<sub>28</sub>- and C<sub>29</sub>-sterols, which was noted following inhibitor treatment. The step-wise  
814 alteration in the sterol compositions observed during a normal excystment-encystment cycle  
815 yielding  $\Delta^5$ -sterols and 6-methyl aromatic sterols from a  $\Delta^{5,7}$ -sterol parent compound is not  
816 consistent with the limited sterol diversity in protozoa, rather it supports a simple model of  
817 cryptic unikont evolution not necessarily observed in the bikont amoeba *Naegleria* wherein a  $\Delta^{5,7}$   
818 -sterol biosynthetic renewal is crucial to trophozoite proliferation,  $\Delta^5$ -sterol synthesis is essential  
819 for the production of a resting cyst capable of excystment and 6-methyl aromatic sterols, derived  
820 from  $\Delta^{5,7}$ -sterols in encysted cells considered non-viable for excystment, promote cell lysis and  
821 death as outlined in the proposed model of *Acanthamoeba* sterol biosynthesis and function  
822 shown in Figure 9.

823 Comparing the ontogenetically regulated sterol compositions in trophozoites and encysted cells  
824 and catalytic analysis of relevant chokepoint enzymes *AcCYP51* and *AcSMT* is phylogenetically  
825 interesting yet connects to the functional importance of sterol products through modified  
826 structural features that occur in the stage-specific furnished molecule. Thus, proliferating  
827 trophozoites synthesize C<sub>28</sub>- and C<sub>29</sub>- $\Delta^{5,7}$ -sterol products typical of kinetoplastids, such as  
828 *Trypanosma cruzi*, and the green algae synthesize ergosterol and 7-dehydroporiferasterol [19, 20,  
829 57] but these organisms synthesize the C<sub>28</sub>- and C<sub>29</sub>-sterols through different biosynthesis routes.  
830 It appears *AcCYP51* possesses substrate preference and catalytic competence more like that of  
831 plant, and hence protozoa, than of fungal or human CYP51 [6]. The substrate specificity of  
832 *AcCYP51* places C14-demethylation after the first sterol methylation step (Fig. 6). However,  
833 while *T. cruzi* has a single SMT1 which is  $\Delta^{24(25)}$  - and  $\Delta^{24(28)}$  -substrate bifunctional capable of  
834 generating a single  $\Delta^{24(28)}$ -Z ethylidene C<sub>29</sub> - product [55-57] and green alga SMT is substrate  
835 bifunctional capable of generating a single  $\Delta^{25(27)}$ -C<sub>29</sub>-sterol product [8], *A. castellanii* has two  
836 SMTs to carry out these sterol methylations at C24 with the second methylation step yielding the  
837 24 $\beta$ -stereochemistry. As we discovered in this investigation through isotopically labeling studies  
838 to amoeba, the *AcSMT2* (or 28-SMT) can, unlike the *T. cruzi* SMT1, synthesize the C<sub>29</sub>- $\Delta^{25(27)}$  -  
839 olefin outcome and the resulting intermediate is precursor to the 7-dehydroporiferasterol and  
840 poriferasterol. Fungi, on the other hand, synthesize a single SMT1 operating the  $\Delta^{24(28)}$  -route  
841 specific for zymosterol and ergosterol while land plants possess two SMTs and both operate the  
842  $\Delta^{24(28)}$  -route such that separate intermediates are involved in the formation of C<sub>28</sub> $\alpha$ -campesterol

843 and C<sub>29</sub>α-sitosterol, respectively [20]. The lineage-specific recurrence of an ancient Δ<sup>25(27)</sup>-sterol  
844 metabolic pathway affording primitive 24β-ethyl sterols in the unikonts suggest divergence with  
845 the ancestral SMT occurred independently multiple times during the course of eukaryote  
846 evolution and within the protozoa product-specific families of SMTs evolved unique to the  
847 Acanthamoeba. The notion of divergent evolution rather than convergent evolution for the  
848 amoeba SMTs is supported by the conservation of sequence similarity and gene structure among  
849 the diverse SMTs isolated throughout the eukaryotic domain to date [8, 59, 60].

850 The results of studies carried out so far on stage-specific sterol profiling in Acanthamoeba and  
851 for GL7 growth responses to sterol supplementation lead to the important conclusion that the  
852 membranes of trophozoites and resting cysts have certain structural requirements for sterol that  
853 are remarkably similar to yeast. They are clearly associated with the three-dimensional character  
854 of the molecule since C<sub>28</sub>- and/or C<sub>29</sub>-sterols are consistently found in the cells. In the  
855 trophozoite and resting cyst, the sterols possess a double bond in ring B of Δ<sup>5,7</sup>-bond  
856 (trophozoite) or Δ<sup>5</sup>-bond (resting cyst). The terminal formation of Δ<sup>5</sup>- sterols could represent a  
857 fine tuning in nucleus planarity but the structural change does not qualify for a significant effect  
858 on membrane fluidity. We surmise the conserved metabolism of Δ<sup>5,7</sup>-sterols to form a Δ<sup>5</sup>-sterol  
859 relates to its homoallylic effect on the C-O bond at C3. For the Δ<sup>5</sup>-sterol, donation of electrons  
860 through an inductive effect, analogously to the well-studied 3,5-cyclosteroid rearrangement,  
861 should strengthen the H-O bond and therefore weaken somewhat and fine-tune any hydrogen  
862 bonding of the sterol to phospholipid in the lipid leaflet of the resting cyst. It should be  
863 remembered that steric interference from C4-methyl groups on the hydrogen bonding ability of  
864 C3- group can weaken sterol-lipid interactions and therefore is reason for removal of C4 to  
865 generate an acceptable sterol membrane insert.

866 In depending upon Δ<sup>5,7</sup>-sterols to act as the encysted cell sterols, it is important not to overlook  
867 these cells are on a trajectory for lysis and death, which associate with rapid turnover of the Δ<sup>5,7</sup>-  
868 sterol, now as intermediates, to a 6-methyl aromatic sterol; cell death from these sterols is  
869 observed in GL7 growth experiments as well. The B-ring aromatic sterols effectively replace  
870 Δ<sup>5,7</sup>-sterols as the membrane component. It appears the architectural unsuitability of the  
871 phenanthrene sterols stems mainly from their diminished hydrogen-bonding strength of the C3-  
872 group resulting from the altered electronegativity of the polar group affected by the double bond

873 conjugations in the nearby aromatic ring. This is consistent with their less polar chromatographic  
874 character in TLC observed too for 4-methyl sterols relative to 4-desmethyl sterols. Alternatively,  
875 contribution from the  $\pi$ -lobe negativity in the B-ring could minimize Van der Waals' forces,  
876 disrupting lipid flexibility in the plasmamembrane.

877 Apart from these considerations and relevant to our research program in rational drug design [27,  
878 33, 58], a major question brought forward by the developmentally regulated sterol biosynthetic  
879 enzymes of *Acanthamoeba* is to what extent they are exploitable by chemotherapy as the relevant  
880 sterol nucleus demethylase enzyme in *Acanthamoeba* differs critically from those of its human  
881 host and the substrate requirements for sterol side chain methylases are unlike any of those for  
882 enzymes in the cholesterol biosynthesis pathway. Thus, the CYP51 and SMT enzymes in  
883 amoeba ergosterol biosynthesis represent potential species-specific drug targets. These enzymes  
884 at MAC concentrations of approximate 1  $\mu\text{M}$  generate trophozoite kill, with the remaining viable  
885 cysts following excystment lysing as the inhibitor pressure continues. Although trophozoite kill  
886 is foremost the focus of our research, prevention of viable cysts that contain brassicaterol and  
887 poriferasterol is also relevant. In the latter case, the possibility for a transcriptional up-regulation  
888 of active  $\Delta^7$ -reductase affecting the conversion of  $\Delta^{5,7}$  - to  $\Delta^5$  -sterol during encystment and its  
889 impairment by an appropriate sterol biosynthesis inhibitor would, in combination therapy with  
890 azole or steroidal inhibitor, enable prevention or cure of diseases from *Acanthamoeba*. It could  
891 be as well the dramatic change in sterol profiles are a combination of anabolic and catabolic  
892 processes since the current study focuses on providing measurements of steady levels of  
893 particular sterols and are not measuring dynamic changes associated with biosynthesis. Further  
894 work is warranted to determine whether additional sterol metabolites or derivatives contribute to  
895 the changes noted in sterol-controlled encystment events and whether their formation are  
896 differentially sensitive to sterol biosynthesis inhibitors.

### 897 *Conclusions.*

898 To summarize the evidence, our findings revealed a new  $\text{C}_{29}$   $\Delta^{25(27)}$  -sterol pathway in protozoa  
899 showing a phylogenetic closeness of *Acanthamoeba* to green alga and provide a powerful  
900 strategy to enhance anti-amoeba efficacy using combinations of azole and steroidal inhibitor to  
901 render resistant amoeba pathogens responsive to ergosterol biosynthesis inhibitor treatment. The  
902 capacity of steroidal inhibitors yet to be discovered (e.g.,  $\Delta^7$ -reductase inhibitor) to modulate

903 core encystation pathway yielding non-viable cells destined to die overcomes a major challenge  
904 for small molecule efficacy against the cysticidal effects of drugs necessary to prevent recurrence  
905 of the disease. The potency of tight binding inhibitors against *A. castellanii* target enzymes was  
906 confirmed by time-kill curves and through encystment-excystment assays. Finally, strict  
907 structural specificities for  $\Delta^{5,7}$ - and  $\Delta^5$ -sterols in the autophagic stage of encystment correlated to  
908 altered membrane structures of encysted cells yielding non-viable or viable cysts; the 6-methyl  
909 aromatic sterols represent chemical signatures for amoeba death accordingly these compounds  
910 can be medical diagnostics.

### 911 **Transparency Document**

912

### 913 **Acknowledgements**

914 This work was supported by the National Institutes of Health Grant R21(R33) AI119782  
915 (WDN). Its contents are solely the responsibility of the authors and do not necessarily represent  
916 the official views of the National Institutes of Health.

917

### 918 **Appendix A. Supplemental Data**

919

920

921

922

923

924

925

926



927 **REFERENCES**

- 928 [1]. Nes, W. D. Biosynthesis of cholesterol and other sterols. *Chem. Rev.* 111 (2011) 6423-6451.
- 929 [2]. Benveniste, P. Biosynthesis and accumulation of sterols. *Annu. Rev. Plant Biol.* 55 (2004)  
930 429-457.
- 931 [3]. Nes, W. R. & McKean, M. L. *Biochemistry of Steroids and Other Isoprenoids*. University  
932 Park Press, Baltimore (1977) pp 325-555.
- 933 [4]. Kodner, R. B. Sterols in a unicellular relative of the metazoans. *Proc. Natl. Acad. Sci. USA*  
934 105 (2008) 9897-9902.
- 935 [5]. Nes, W.R. and Nes, W. D. *Lipids in Evolution*. Plenum Press, New York (1980).
- 936 [6]. Hargrove, T. Y., et al. Substrate preferences and catalytic parameters determined by  
937 structural characteristics of sterol 14 $\alpha$ -demethylase CYP51 from *Leishmania infantum*. *J. Biol.*  
938 *Chem.* 286 (2011) 26838-26848.
- 939 [7]. Bloch, K. E. Sterols structure and membrane function. *CRC Crit. Rev. Biochem.* 14 (1983)  
940 47-82.
- 941 [8]. Nes, W. D. et al. The structural requirements of sterols for membrane function in  
942 *Saccharomyces cerevisiae*. *Arch. Biochem. Biophys.* 300 (1993) 724-733.
- 943 [9]. Lepesheva, G. I. et al. Sterol 14 $\alpha$ -demethylase inhibitors as potential target for  
944 antitrypanosomal therapy: Enzyme inhibition and parasite growth. *Chem. & Biol.* 14 (2007) 1-  
945 11.
- 946 [10]. De Souza, W. & Fernandes Rodrigues, J. C. Sterol biosynthesis pathway as target for anti-  
947 trypanosomal drugs. *Interdisciplin. Perspect. Infect. Dis.* 2009 (2009) 1-19.
- 948 [11]. Bloch, K. E. *Blondes in Venetian Paintings, the Nine-Banded Armadillo, and other Essays*  
949 *in Biochemistry*, Yale University Press, New Haven (1994).
- 950 [12]. Ourisson, G. and Nakatani. The terpenoid theory of the origin of cellular life: the evolution  
951 of terpenoids to cholesterol. *Chem. Biol.* 1 (1994) 11-23.
- 952 [13]. Summons, R. E. et al. Steroids and triterpenoids and molecular oxygen. *Phil. Trans. R. Soc.*  
953 361 (2006) 951-968.
- 954 [14]. Knoll, A H. Paleobiological perspectives on early eukaryotic evolution. In *The Origin and*  
955 *Evolution of Eukaryotes*, (Keeling, P. J and Koonin, E. V, eds). Cold Spring Harbor Laboratory  
956 Press. (2014) pp 1-14.
- 957 [15]. Desmond, E. and Gribaldo, S. Phylogenomics of sterol synthesis: Insights into the origin,  
958 evolution and diversity of a key eukaryote feature. *Genome Biol. Evol.* 1 (2011) 364-381.
- 959 [16]. Gold, D. A. et al. Paleoproterozoic sterol biosynthesis and the rise of oxygen. *Nature* 543  
960 (2017) 420-423.

- 961 [17]. Rezen, T. et al. New aspects on lanosterol 14 $\alpha$ -demethylase and cytochrome P450  
962 evolution: Lanosterol/cycloartenol diversification and lateral transfer. *J. Mol. Evol.* 59 (2004)  
963 51-58 (2004).
- 964 [18]. Wei, J. H., Yin, X., Welander, P. V. Sterol synthesis in diverse bacteria. *Front. Microbiol.* 7  
965 (2016) 1-19.
- 966 [19]. Miller, M. B. et al. Evolutionarily conserved  $\Delta^{25(27)}$ -ergosterol biosynthesis pathway in the  
967 alga *Chlamydomonas reinhardtii* is distinct from the  $\Delta^{24(28)}$ -pathway to fungal ergosterol. *J. Lipid*  
968 *Res.* 53 (2012) 1636-1645.
- 969 [20]. Haubrich, B. A. et al. Characterization, mutagenesis and mechanistic analysis of an ancient  
970 algal sterol C24-methyltransferase: Implications for understanding sterol evolution in the green  
971 lineage. *Phytochemistry* 113 (2015) 64-72.
- 972 [21]. Garg, V. K. Nes, W. R. Changes in  $\Delta^5$  – and  $\Delta^7$ - sterols during germination and seedling  
973 development of *C. maxima*. *Lipids* 20 (1985) 876-884.
- 974 [22]. Guo, D., Venkatramesh, M Nes, W. D. Developmental regulation of sterol biosynthesis in  
975 *Zea mays*. *Lipids* 30 (1996) 203-219.
- 976 [23]. Neff, RJ, Ray, SA, Benton, WF, Wilborn, M. Chapter 4 Induction of synchronous  
977 encystment (differentiation) in *Acanthamoeba sp.*, In: DM Prescott, Editor(s), *Methods in Cell*  
978 *Biology*, Academic Press, Vol. 1 (1964) pp 55-83.
- 979 [24]. Bowers, B, Korn, E. D. The fine structure of *Acanthamoeba castellanii* (Neff strain). *J Cell.*  
980 *Biol.* 41 (1969) 786-805.
- 981 [25]. Moon E-K, Kim, S-E, Hong Y, Chung D-II, Goo, Y-K, Kong, H-H. Autophagy inhibitors  
982 as a potential anti-amoebic treatment for *Acanthamoeba keratitis*. *Antimicrob. Agents*  
983 *Chemotherap.* 59 (2015) 4020-4025.
- 984 [26]. Martin-Navarro, CM, et al. Statins and voriconazole induce programmed cell death in  
985 *Acanthamoeba castellanii*. *Antimicrob. Agents Chemotherap.* 59 (2015) 2817-2824.
- 986 [27]. Haubrich, B. A., et al. Discovery of an ergosterol-signaling factor that regulates  
987 *Trypanosoma brucei* growth. *J. Lipid Res.* 56 (2015) 331-341.
- 988 [28]. Raederstorff, D., Rohmer, M. Sterol biosynthesis de novo via cycloartenol by the soil  
989 amoeba *Acanthamoeba polyphaga*. *Biochem. J.* 231 (1985) 609-6015.
- 990 [29]. Raederstorff, D., Rohmer, M. The action of the systemic fungicides tridemorph and  
991 fenpropimorph on sterol biosynthesis by the soil amoeba *Acanthamoeba polyphaga*. *Eur. J.*  
992 *Biochem.* 164 (1987) 421-426.
- 993 [30]. Korn, E.D., et al The enzymatic aromatization of the B-ring of  $\Delta^{5,7}$ -sterol. *Biochim.*  
994 *Biophys. Acta.* 187 (1969) 553-563.
- 995 [31]. Bisseret, P, Adam, H, Rohmer, M. Structural elucidation of ring-B aromatic sterols of the  
996 soil amoeba *Acanthamoeba polyphaga*. *J. Chem. Soc. Chem. Commun.* (1987) 693-695.

- 997 [32]. Lamb, D.C., et al. Azole antifungal agents to treat the human pathogens *Acanthamoeba*  
998 *castellani* and *Acanthamoeba polyphaga* through inhibition of sterol 14-demethylase (CYP51).  
999 Antimicrob. Agents Chemother. 59 (2015) 4707-4713.
- 1000 [33]. Kildane, M.E., et al. Sterol methyltransferase a target for anti-amoeba therapy: Towards  
1001 transition state analog and suicide substrate design. J. Lipid Res. 58 (2017) 2310-2323.
- 1002 [34]. Thomson, S., et. al. Characterisation of sterol biosynthesis and validation of 14 $\alpha$ -  
1003 demethylase as a drug target in *Acanthamoeba*. Sci. Rep. 7 (2017) 1-9.
- 1004 [35]. Mehdi, H, Garg, NK. Changes in the lipid composition and activities of isocitrate  
1005 dehydrogenase and isocitrate lyase during encystation of *Acanthamoeba culbertsoni* strain A1.  
1006 Trans. R. Soc. Tropical Med. Hygen. 81 (1987) 633-636.
- 1007 [36]. Zhou, W., Lepesheva, G. I., Waterman, M. R. Nes, W. D. Mechanistic analysis of a  
1008 multiple product sterol methyltransferase from *Trypanosoma brucei* implicated in ergosterol  
1009 biosynthesis.. J. Biol. Chem. 281 (2006) 6290-6296.
- 1010 [37]. Xu, S., Norton, R. A., Crumley, F. G. Nes, W. D. Comparison of the chromatographic  
1011 properties of sterols, select additional steroids and triterpenoids: Gravity-flow liquid  
1012 chromatography, thin-layer chromatography, gas-liquid chromatography, and high performance  
1013 liquid chromatography. J. Chromatogr. 452 (1988) 377-398.
- 1014 [38]. Copeland, R. A. Enzymes 2<sup>nd</sup> Edition Wiley-VCH New York (2000).
- 1015 [39]. Ramgopal, M., Bloch, K. Sterol syngerism in yeast. Proc. Natl. Acad. 80 (1983) 712-715.
- 1016 [40]. Smith, F. R. Korn, E. D. 7-Dehydrostigmasterol and ergosterol: The major sterols of an  
1017 amoeba. J. Lipid Res. 9 (1968) 405-408.
- 1018 [41]. Nes, W. D., et al. Concerning the role of 24,25-dihydrolanosterol and lanostanol in sterol  
1019 biosynthesis by cultured cells. Steroids 53 (1988) 461-475.
- 1020 [42]. Taton, M and Rahier, A. Properties and structural requirements for substrate specificity of  
1021 cytochrome P450-dependent obtusifoliol 14- $\alpha$  demethylase from maize (*Zea mays*)  
1022 seedlings. Biochem. J. 277 (1990) 483-492.
- 1023 [43]. Bellamine, A., et al. Structural requirements for substrate recognition of Mycobacterium  
1024 tuberculosis 14 $\alpha$ -demethylase: implications for sterol biosynthesis. J. Lipid Res. 42 (2001) 128-  
1025 136.
- 1026 [44] Nes, W. D., et al. 9 $\beta$ ,19-Cyclosterol analysis by <sup>1</sup>H- and <sup>13</sup>C-NMR, crystallographic  
1027 observations and molecular mechanics calculations. J. Amer. Chem. Soc. 120 (1998) 5970-5980.
- 1028 [45] Gas-Pascual, E. et al. Plant oxidosqualene metabolism: Cycloartenol synthase-dependent  
1029 sterol biosynthesis in *Nicotiana benthamiana*. PlosOne 9 (2014) 1-9.
- 1030 [46]. Goad, L.J and Akihisa, T. Analysis of Sterols. Blackie Academic, London 1997 437 pp.
- 1031 [47] Zhou, W., Cross, G. A. M., Nes, W. D. J. Lipid Res. 48 (2007) 665-673.

1032 [48] Nes, W. D., Heupel, R.C. Le, P. H. Biosynthesis of ergosta-6(7),8(14),22(23)-trien-3 $\beta$ -ol by  
1033 *Gibberella fujikuroi*: Its importance to ergosterol's biosynthesis pathway. Chem. Commun.  
1034 (1985) 1431-1433.

1035 [49] Muller, C., Binder, U., Bracher, F. Giera, M. Antifungal drug testing by combining minimal  
1036 inhibitory concentration testing with target identification by gas chromatography-mass  
1037 spectroscopy. Nat. Protocols 12 (2017) 947-963.

1038 [50] Mehdi, H. Sterols of *Acanthamoeba culbertsoni* strain A-1. Steroids 551 (1988) 551-558.

1039 [51]. Nes, W. R. Biochemistry of plant sterols. Adv. Lipid Res. 15 (1977) 233-359.

1040 [52]. Roti, L. W. Stevens, A. R. Effect of 5-bromodeoxyuridine on growth, encystment, and  
1041 encystment of *Acanthamoeba castellanii*. J. Cell Biol. 61 (1974) 233-237.

1042 [53] Nes, W. R. Dhanuka, I. C. Inhibition of sterol synthesis by  $\Delta^5$ -sterols in a sterol auxotroph  
1043 of yeast defective in oxidosqualene cyclase and cytochrome P-450. J. Biol. Chem. 263 (1988)  
1044 11844-11850.

1045 [54]. Roberts, C. W. R. et al. Fatty acid and sterol metabolism: potential antimicrobial targets in  
1046 apicomplexan and trypanosomatid parasitic protozoa. Mol. Biochem. Parasitol. 126 (2003) 129-  
1047 142.

1048 [55]. Urbina, J. A. et al. Modification of the sterol composition of *Trypanosoma*  
1049 (*Schizotrypanum*) *cruzi* epimastigotes by D24(25)-sterol methyltransferase inhibitors and their  
1050 combinations with ketoconazole. Mol. Biochem. Para. 34 (1995) 199-210.

1051 [56]. Sowa, M. A. Characterization and inhibition of C24-sterol methyltransferase of  
1052 *Trypanosoma cruzi*. Master of Science, Texas Tech University (2016) 1-65.

1053 [57]. Sterol methyltransferase enzyme and its chemotherapeutic implications for Chagas disease.  
1054 Doctoral Dissertation, Texas Tech University (2014) 1-76.

1055 [58]. Kanagasabai, R., et al. Disruption of ergosterol biosynthesis, growth and the morphological  
1056 transition in *Candida albicans* by sterol methyltransferase inhibitors containing sulfur at C-25 in  
1057 the sterol side chain. Lipids, 39 (2004) 737-746.

1058 [59]. Gold, D. A. et al. Sterol and genomic analyses validate the sponge biomarker hypothesis.  
1059 Proc. Natl. Acad. Sci. USA 113 (2016) 2684-2689.

1060 [60]. Neelakandan, A. K. et al. Cloning, functional expression, and phylogenetic analysis of plant  
1061 24C-methyltransferases involved in sitosterol biosynthesis. Phytochemistry, 70 (2009) 1982-  
1062 1998.

1063

1064

1065

1066

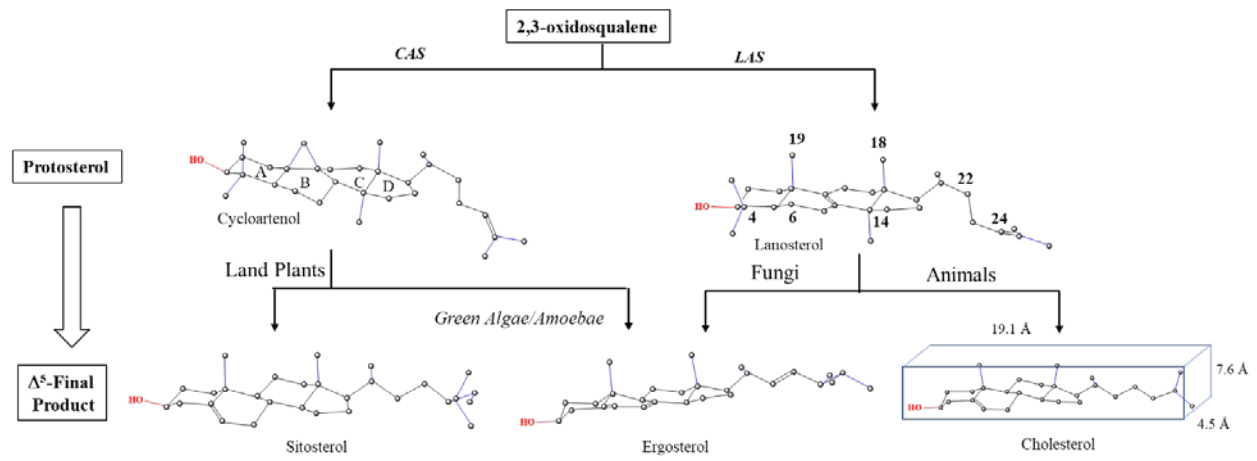
1067

1068

1069

1070

1071



1072

1073 **Figure 1.** Sterol biosynthesis diversity in eukaryote organisms.

1074

1075

1076

1077

1078

1079

1080

1081

1082

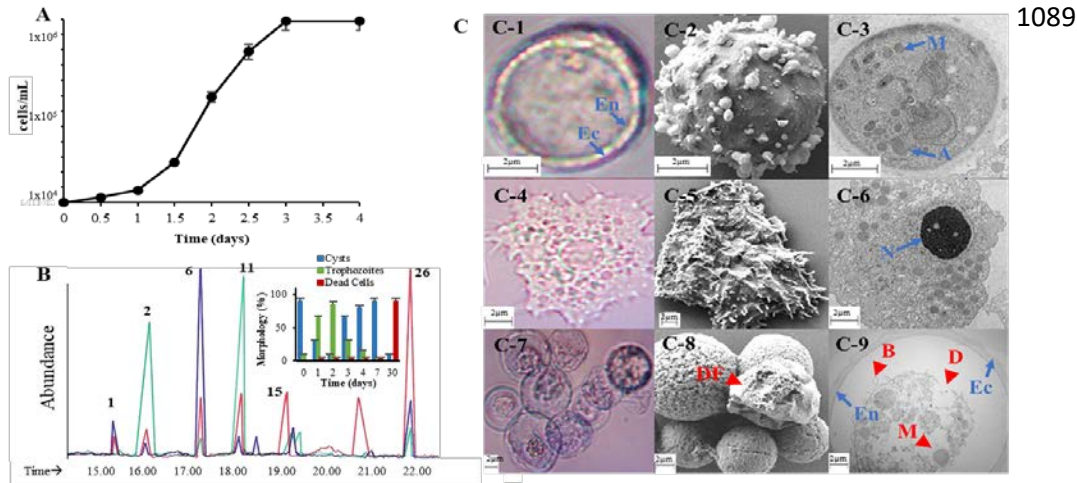
1083

1084

1085

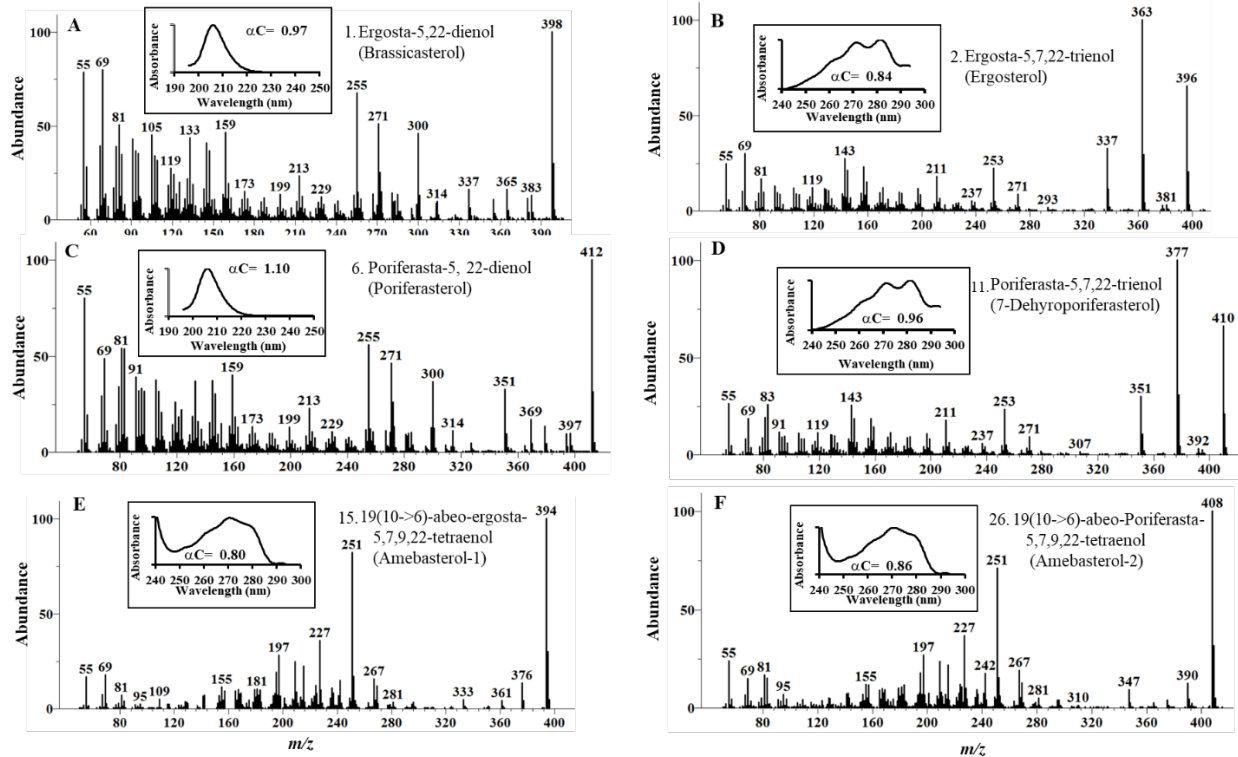
1086

1087



1090

1091 **Figure 2.** Developmental changes in *A. castalenii* growth and sterol biosynthesis. Panel A,  
 1092 Proliferation of trophozoites from a true cyst inoculum. Panel B, Total ion current  
 1093 chromatograms of neutral lipids of trophozoites (green), true (viable) cysts (blue) and dead cells  
 1094 (red); GC peaks correspond to 1= brassicasterol, 2=ergosterol, 6=poriferasterol, 11=7-  
 1095 dehydroporiferasterol, 15= amebasterol-1 and 26 = amebasterol; inset shows quantitative  
 1096 changes in the population of encysted cells to trophozoite to dead cells. Panel C, C1-light  
 1097 micrograph (LM) of double wall viable cyst used as inoculum with rounded outer wall ectocyst  
 1098 (EC) and inner wall endocyst (EN), C2-scanning electron micrograph (SEM) of cyst in the  
 1099 process of excystment., C3- Transmission electron micrograph (TEM) of true cyst showing  
 1100 diagnostic mitochondria (M) and autolysosomes (A). C4-LM of trophozoite, C5-SEM of  
 1101 trophozoite showing acanthopodia. C6 TEM of trophozoite showing prominent central  
 1102 nucleolous (n), mitochondria and cytoplasmic food vacuoles. C7-LM of trypan blue stained  
 1103 clumped encysted cells showing many dead. C8- SEM of clumped encysted cells of control or  
 1104 25-azacycloartenol treated trophozoites showing deflated (DF) cell characteristic of dead cells.  
 1105 L9- TEM of encysted trophozoite from L8 samples showing ectocyst-endocyst boundary and  
 1106 abnormal morphological features of autophagy-like structures that contain undigested organelles  
 1107 (arrow), blebby structures in the membranes (B, arrowheads) and disorganized membrane  
 1108 structures (D, arrowhead), intense vacuolization and loss of mitochondria.



1109

1110 **Figure 3.** Chromatographic and spectral characteristics of main *Acanthamoeba* sterols from the  
 1111 growth studies shown in Figure 2.

1112

1113

1114

1115

1116

1117

1118

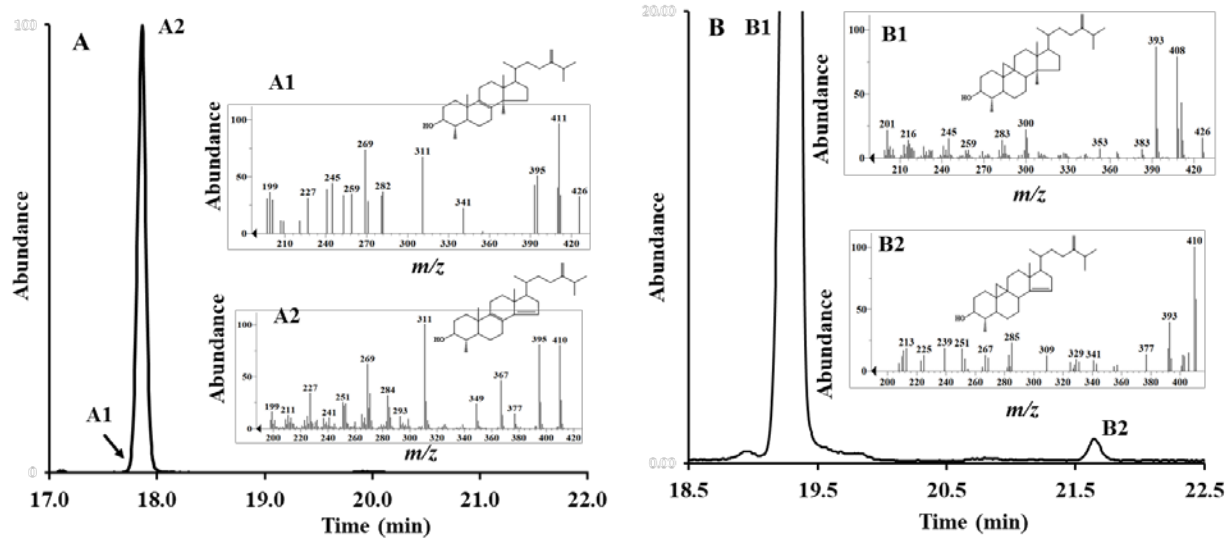
1119

1120

1121

1122





1123

1124 **Figure 4.** GC-MS analysis of the AcCYP51-generated products. (A) The total ion current  
 1125 chromatogram (insert- mass spectra of relevant GC peaks) of incubation with obtusifoliol. (B)  
 1126 The total ion current chromatogram (insert-mass spectra of relevant GC peaks) of incubation  
 1127 with cycloeucaleanol.

1128

1129

1130

1131

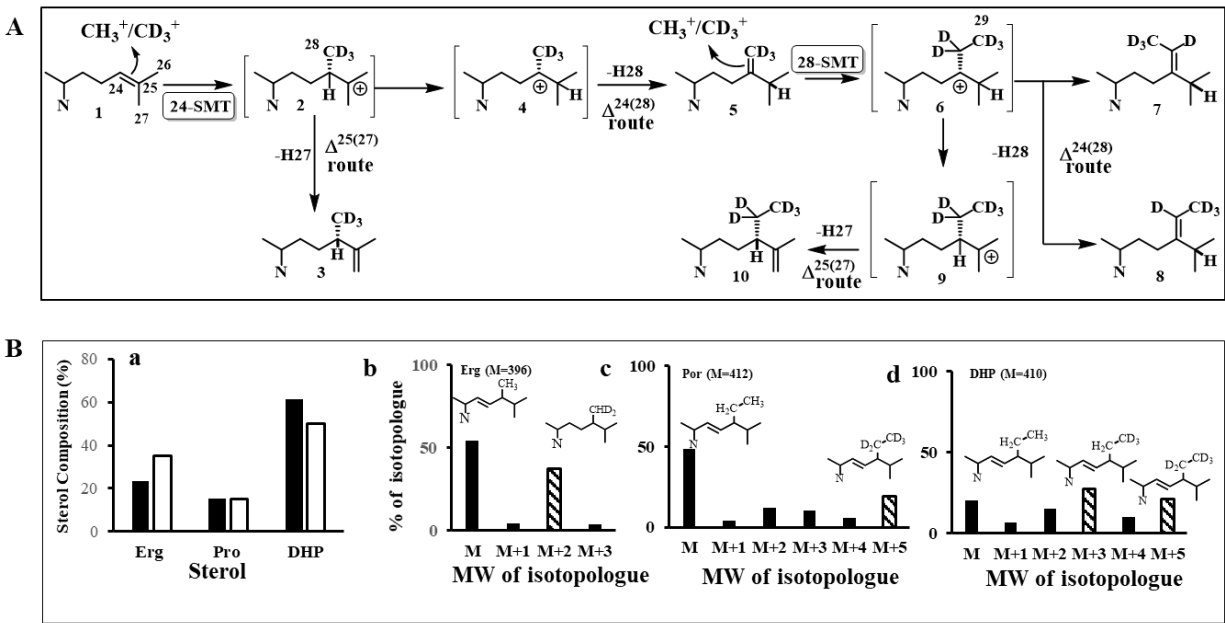
1132

1133

1134

1135

1136



1137

1138 **Figure 5.** Sterol C24-methylation activity in *Acanthamoeba*. (A) Proposed sterol C24-  
 1139 methylation pathway in *Acanthamoeba* showing incorporation of SAM and [*methyl*-<sup>2</sup>H<sub>3</sub>]SAM =  
 1140 D<sub>3</sub>-SAM at C24 and C28 of the sterol side chain. (B) Mass spectral analysis of sterols  
 1141 (ergosterol, erg, poriferasterol, por, and 7-dihydroporiferasterol, DHP) recovered from  
 1142 trophozoites incubated in the presence and absence of [*methyl*-<sup>2</sup>H<sub>3</sub>]methionine.

1143

1144

1145

1146

1147

1148

1149

1150

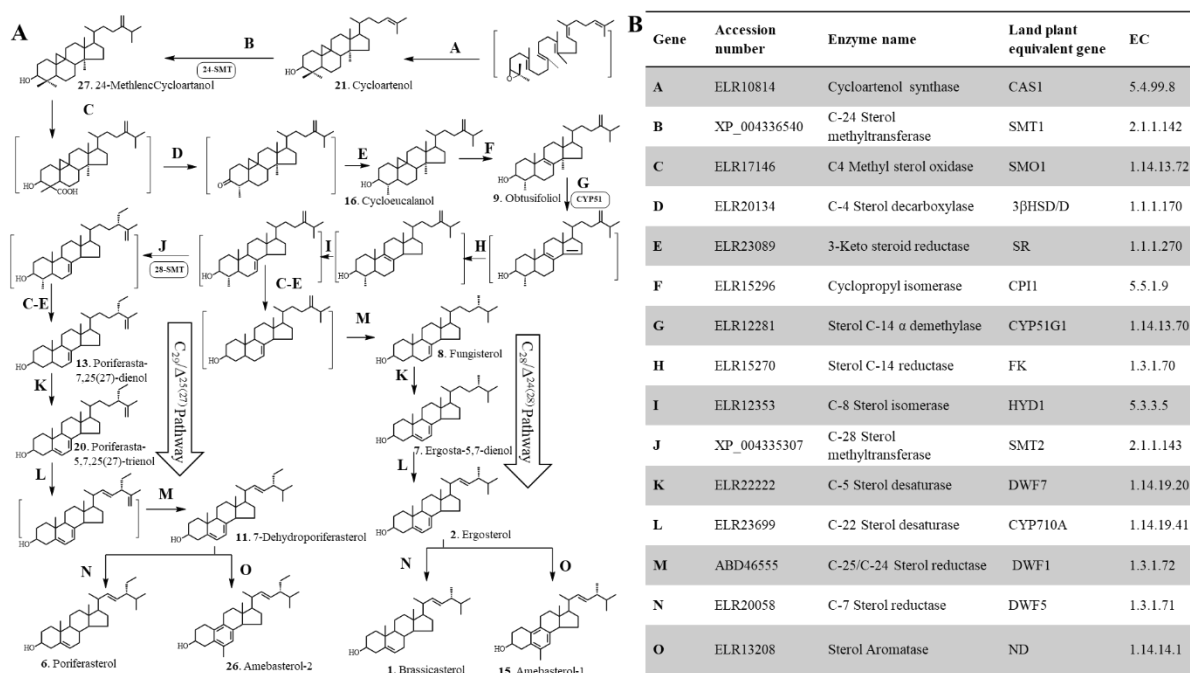
1151

1152

1153

1154

1155



1156

1157 **Figure 6.** Biosynthetic model for the formation of phytosterols in *Acanthamoeba*. (A) Proposed  
 1158 separate  $\Delta^{24(28)}$  - and  $\Delta^{25(27)}$  -olefin intermediates to  $C_{28}$ - and  $C_{29}$ -sterol products. (B). Sterolic  
 1159 genes identified in the Ac Genebank compared to known sterolic genes from land plants and  
 1160 humans (aromatase).

1161

1162

1163

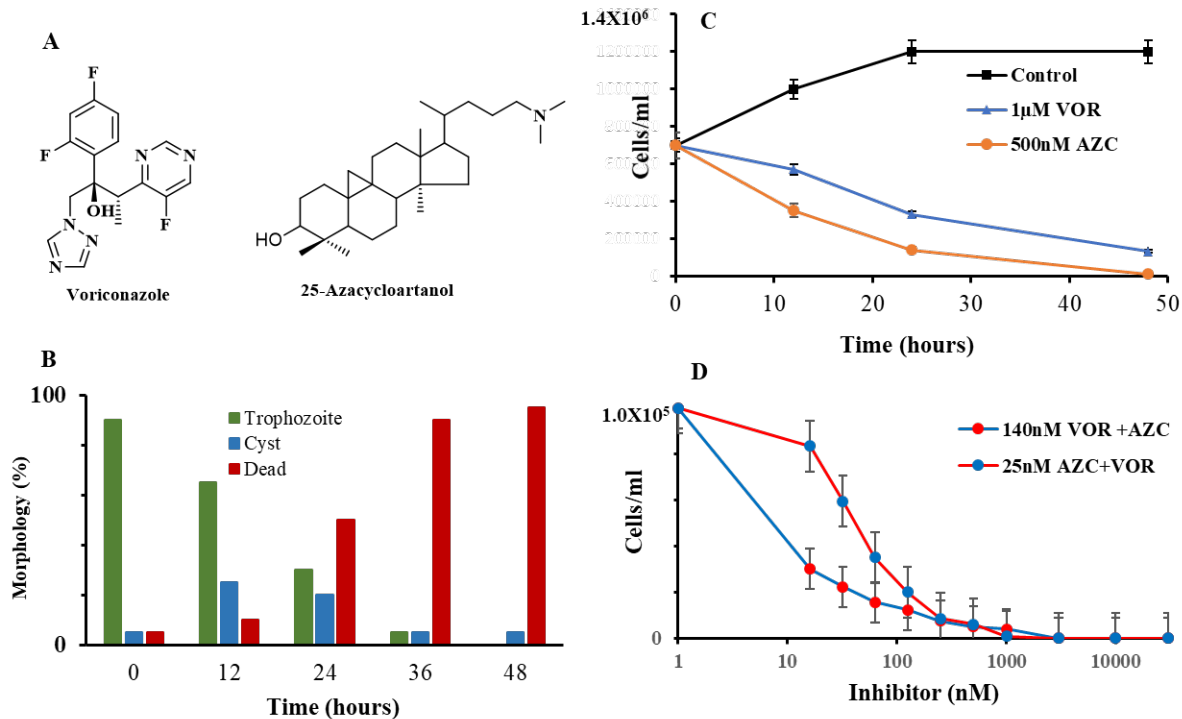
1164

1165

1166

1167

1168

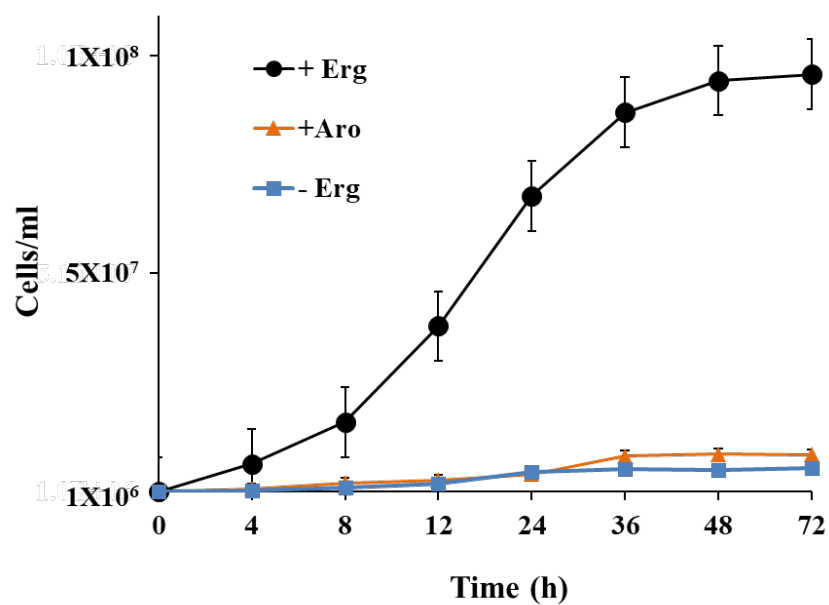


1169  
 1170 **Figure 7.** Effects of ergosterol biosynthesis inhibitors as single or combination treatment on  
 1171 *Acanthamoeba* growth and encystment prepared by Method-1 (Materials and Methods). Panel A,  
 1172 structures of growth inhibitors. Panel B, Time-kill studies of 25-azacycloartanol (AZC) and  
 1173 voriconazole (VOR). Panel C, Quantification of AZC treated cysts (viable and clumped non-  
 1174 viable) and dead cells determined microscopically and by trypan blue staining. Panel D. *A.*  
 1175 *castellanii* treated with VOR and AZC at the previously determined IC<sub>50</sub> concentration and then  
 1176 using the pair of compounds at varied concentration of the inhibitor from 16 nM to 3  $\mu$ M. Data  
 1177 represent mean  $\pm$ sd. P < 0.05, determined by T-test. In each case data are from a single  
 1178 experiment which is representative of three independent experiments.

1179  
 1180  
 1181  
 1182  
 1183  
 1184  
 1185  
 1186  
 1187

1188

1189

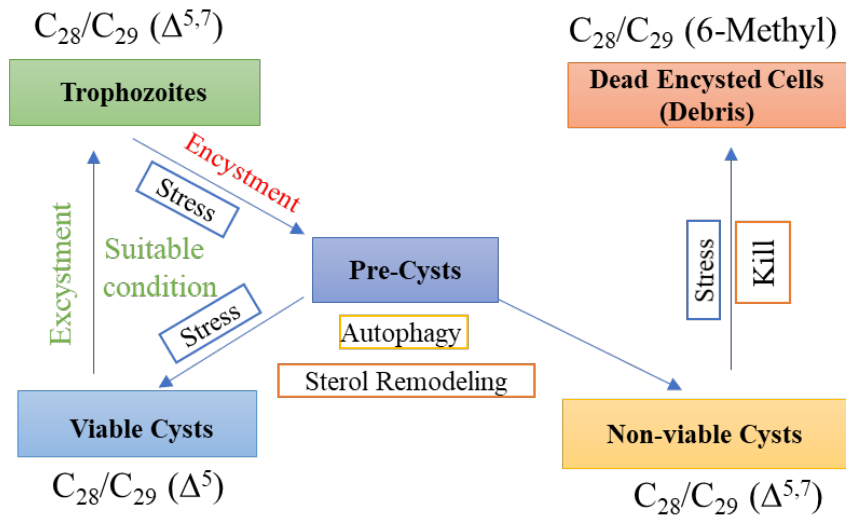


1190

1191 **Figure 8.** *Saccharomyces cerevisiae* strain GL7 defective in ergosterol biosynthesis incubated  
1192 with nutritional sterols supplements as described in Materials and Methods; ergosterol (black  
1193 circle), 6-methyl sterol aromatics from *A. castellanii* (orange circle) or no sterol (blue circle).  
1194 Note, 7-dehydroporiferasterol, brassicasterol and poriferasterol supplements supported growth in  
1195 similar fashion to ergosterol-grown cells.

1196

1197



1198

1199 **Figure 9.** Proposed model for stage-specific sterols in growth and encystment leading to  
1200 alternate trajectories for the production of viable or non-viable cysts.

1201

1202

1203